Original article

MOLECULAR METABOLISM

α-Melanocyte stimulating hormone promotes muscle glucose uptake via melanocortin 5 receptors

Pablo J. Enriori [1,11], Weiyi Chen [1,11], Maria C. Garcia-Rudaz [1,9], Bernadette E. Grayson [2,10], Anne E. Evans [2], Sarah M. Comstock [2], Ursel Gebhardt [3], Hermann L. Müller [3], Thomas Reinehr [4], Belinda A. Henry [1], Russell D. Brown [1], Clinton R. Bruce [1], Stephanie E. Simonds [1], Sara A. Litwak [1], Sean L. McGee [5], Serge Luquet [6], Sarah Martinez [6], Martin Jastroch [7], Matthias H. Tschöp [7], Matthew J. Watt [1], Iain J. Clarke [1], Christian L. Roth [8], Kevin L. Grove [2], Michael A. Cowley [1,*]

ABSTRACT

Objective: Central melanocortin pathways are well-established regulators of energy balance. However, scant data exist about the role of systemic melanocortin peptides. We set out to determine if peripheral α-melanocyte stimulating hormone (α-MSH) plays a role in glucose homeostasis and tested the hypothesis that the pituitary is able to sense a physiological increase in circulating glucose and responds by secreting α-MSH.

Methods: We established glucose-stimulated α-MSH secretion using humans, non-human primates, and mouse models. Continuous α-MSH infusions were performed during glucose tolerance tests and hyperinsulinemic-euglycemic clamps to evaluate the systemic effect of α-MSH in glucose regulation. Complementary *ex vivo* and *in vitro* techniques were employed to delineate the direct action of α-MSH via the melanocortin 5 receptor (MC5R)—PKA axis in skeletal muscles. Combined treatment of non-selective/selective phosphodiesterase inhibitor and α-MSH was adopted to restore glucose tolerance in obese mice.

Results: Here we demonstrate that pituitary secretion of α-MSH is increased by glucose. Peripheral α-MSH increases temperature in skeletal muscles, acts directly on soleus and gastrocnemius muscles to significantly increase glucose uptake, and enhances whole-body glucose clearance via the activation of muscle MC5R and protein kinase A. These actions are absent in obese mice, accompanied by a blunting of α-MSH-induced cAMP levels in skeletal muscles of obese mice. Both selective and non-selective phosphodiesterase inhibition restores α-MSH induced skeletal muscle glucose uptake and improves glucose disposal in obese mice.

Conclusion: These data describe a novel endocrine circuit that modulates glucose homeostasis by pituitary α-MSH, which increases muscle glucose uptake and thermogenesis through the activation of a MC5R-PKA-pathway, which is disrupted in obesity.

Keywords α-MSH; Pituitary; Skeletal muscles; MC5R; PKA; Glucose homeostasis

1. INTRODUCTION

Proopiomelanocortin (POMC) cells are found in the arcuate nucleus of the hypothalamus (ARH), the nucleus of the solitary tract, the pituitary, and the skin (keratinocytes). These cells produce the polypeptide precursor POMC, which is then tissue-specifically modified to generate smaller, active peptides [1]. The POMC system within the brain is important in the regulation of food intake and energy expenditure [2]. The pituitary gland consists of an anterior lobe (AL), an intermediate lobe (IL), and a neural lobe (NL). Within the AL, corticotrophs express POMC, which is processed to produce adrenocorticotropic hormone (ACTH) and minor amounts of β-lipotrophin, β-endorphin (β-end), and

[1]Biomedical Discovery Institute/Department of Physiology, Monash University, Vic, Australia [2]Division Neuroscience, Oregon Health and Science University, Oregon, USA [3]Department of Pediatrics, Vestische Children Hospital Datteln, University of Witten/Herdecke, Germany [4]Department of Pediatrics, Klinikum Oldenburg GmbH, Germany [5]Metabolic Research Unit, School of Medicine, Deakin University, Vic, Australia [6]Univ Paris Diderot, Sorbonne Paris Cité, Unité de Biologie Fonctionnelle et Adaptative, CNRS UMR 8251, F-75205 Paris, France [7]Institute for Diabetes and Obesity, Helmholtz Zentrum München, German Research Center for Environmental Health, Neuherberg & Division of Metabolic Diseases, Technische Universität, München, Germany [8]Division of Endocrinology, Seattle Children's Hospital Research Institute, WA, USA

[9] Present address: Department of Paediatric, Division of Women, Youth and Children, The Canberra Hospital, ACT, Australia.

[10] Present address: University of Mississippi Medical Center, MI, USA.

[11] Pablo J. Enriori and Weiyi Chen contributed equally to this work.

*Corresponding author. Biomedical Discovery Institute/Department of Physiology, Faculty of Medicine, Nursing and Health Sciences, Monash University, Wellington Road, Clayton, Vic 3800, Australia. E-mail: michael.cowley@monash.edu (M.A. Cowley).

Received May 29, 2016 • Revision received July 26, 2016 • Accepted July 28, 2016 • Available online 5 August 2016

http://dx.doi.org/10.1016/j.molmet.2016.07.009

α-MSH. In the IL, the predominant products are β-end and α-MSH [3,4]. Accordingly, the predominance of circulating α-MSH originates from the IL in most mammals. In the human, however, the IL is rudimentary and most of the circulating α-MSH presumably originates from the AL [3].

Our current understanding of the pituitary indicates that POMC pituitary cells are controlled entirely by the hypothalamic endocrine system and by feedback signals from hypothalamic circuits, the pituitary and specific peripheral organs.

However, it is plausible that direct regulation of AL pituitary cells by blood glucose exists, because glucose-sensing cells are found in the AL of the pituitary [5]. In addition, peripheral α-MSH has been implicated in fatty acid oxidation in skeletal muscle cells through the activation of MC5R [6]. Since then, the peripheral effect of α-MSH has not been tested *in vivo*.

Genetic defects resulting in inactivation of the central and peripheral melanocortin system have been shown to lead to obesity and alteration of glucose homeostasis/insulin sensitivity [7–9]. While most believe this alteration is due to regulation by the CNS, one cannot exclude contributions by tissues of the periphery, especially since α-MSH is detectable in blood and its levels can change depending on different energy states [10,11]. Skeletal muscle plays a major role in determining whole body energy expenditure, accounting for ~30% of resting energy expenditure [12]. Skeletal muscle accounts for 15–20% total glucose disposal in the basal state and 80% under euglycemic hyperinsulinemic conditions [13,14].

We set out to determine if peripheral α-MSH plays a role in glucose homeostasis and tested the hypothesis that the pituitary is able to sense a physiological increase in circulating glucose and responds by secreting α-MSH. We show that glucose stimulates α-MSH production and increases circulating concentrations, which increases muscle glucose uptake through the activation of the MC5R-PKA pathway.

2. RESULTS

2.1. Postprandial α-MSH release

To begin, we employed RIA to specifically detect and quantify α-MSH levels in the plasma after a meal. We found that α-MSH levels in the plasma of rhesus macaques fluctuate between a 5–25 pM range during a 24-h fasting period. With scheduled feeding of a standard low-fat diet, α-MSH levels increased by 2-fold above fasting levels (AUC $p < 0.05$, Figure 1A and B). To determine the relationship between α-MSH release and diet composition, animals received a high caloric diet (HCD), a standard diet (control diet), or no meal after an overnight fast. Caloric intake was higher in the group fed with HCD (2020 ± 378 vs 941 ± 70 cal) and, as shown in Figure 1C, α-MSH levels were significantly increased to 33.3 ± 5.7 pM ($p < 0.001$) after 5 h of HCD feeding compared to 5 h fasting, suggesting that specific components of this diet induced a release of α-MSH into the blood.

2.1.1. α-MSH release from the pituitary is regulated by glucose

Following the postprandial release of α-MSH, we determined the source of α-MSH by assessing α-MSH expression using double immuno-fluorescence with anti-α-MSH/ACTH in Japanese macaque pituitary samples (Figure 2B). A cross-reaction was avoided by pre-absorbing the anti-α-MSH antibody with ACTH and *vice versa*

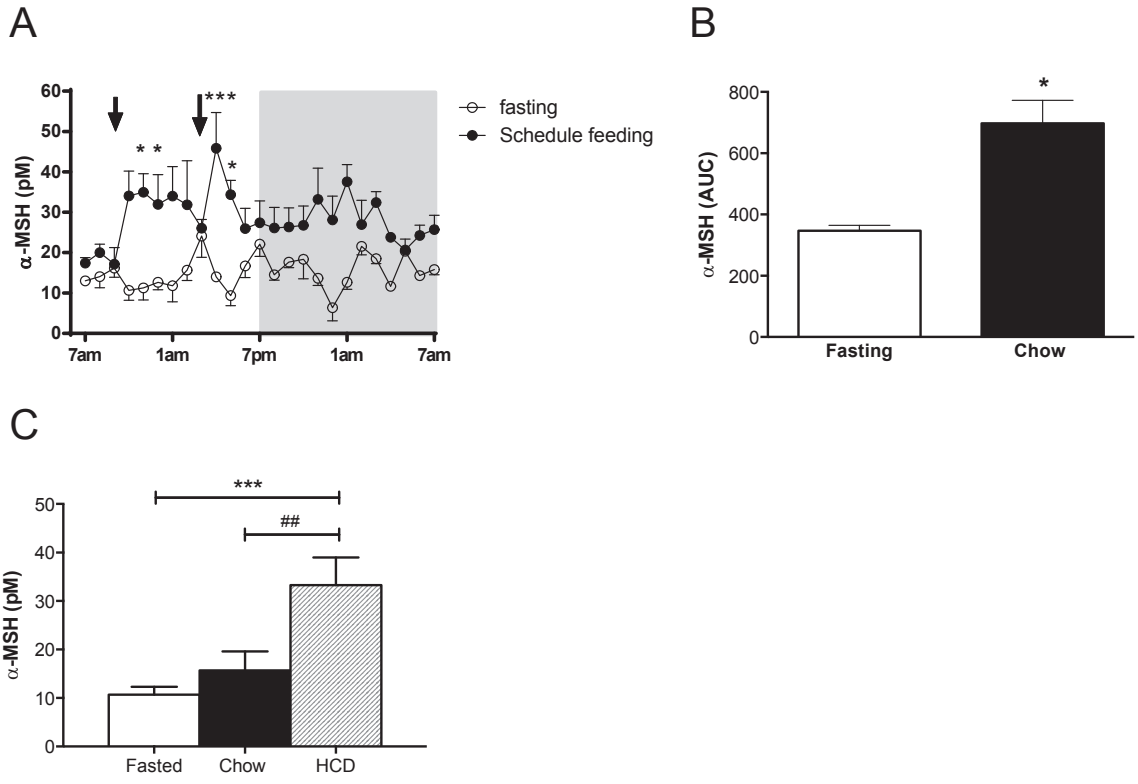

Figure 1: Circulating α-MSH is increased in monkeys after feeding. A. α-MSH levels in plasma of fasting and schedule feeding rhesus macaques ($n = 4$) during 24 h. Arrows represent the times at which monkeys received meals (9 am and 3 pm). The gray shaded area represents the dark period. (*$p < 0.05$ and ***$p < 0.001$ by Two-way ANOVA vs. fasting). B. AUC of α-MSH levels during fasting and schedule feedings (*$p < 0.05$). C. Macaque α-MSH levels 5 h after fasting or eating regular chow or HCD ($n = 6$; ##$p < 0.01$, ***$p < 0.001$). Data are expressed as mean ± SEM.

(Figures 2C and S1). Most of the AL cells were ACTH positive, while some showed co-localization with α-MSH. In contrast, most of the IL cells were double-positive for α-MSH and ACTH. Interestingly, some tightly arranged cells in the IL were observed with high α-MSH immunoreactivity (1300 pmol/mg protein). Additionally, the AL contributed considerably to the α-MSH levels detected (650 pmol/mg protein) (Figure 2A and D).

To bolster the above findings, we investigated α-MSH levels in patients with low- or non-functioning pituitaries, panhypopituitarism (PH), and in patients with craniopharyngioma after surgery (CP). We established that both PH and CP patients had very low plasma α-MSH levels, being 70% lower than healthy subjects with intact pituitary function (Figure 2E). Moreover, plasma α-MSH levels were undetectable (the sensitivity of radioimmunoassay is 0.30 fmol/mL) in about half of the patients, and measurements could be obtained in all healthy controls. Thus far, these results strongly support the pituitary as the main contributor of circulating α-MSH and bring to light a plausible role of α-MSH in glucose regulation.

2.1.2. Glucose regulates circulating α-MSH levels in humans, monkeys and mice

Before delving into the role of α-MSH in glucose regulation, we performed glucose tolerance tests (GTT) in healthy and obese children (oral), lean and obese monkeys (intravenous, iv), and lean and diet induced obese (DIO) mice (intraperitoneal, ip) to examine α-MSH regulation by glucose *in vivo*. As shown in Figure 3A, B, and C, α-MSH levels peaked at 15 min after glucose administration in all species. However, in monkeys, we observed an initial smaller α-MSH peak (5 min), which likely resulted from iv administration causing a far more rapid delivery of glucose to the peripheral tissues. Obese subjects displayed the same pattern of α-MSH response as lean controls (Figure 3A). Obese monkeys had a higher response of α-MSH than controls (Figure 3B). Additionally, we estimated a strong correlation between α-MSH with both blood glucose and plasma insulin levels (AUC, Figures S3A and S3B), supporting the hypothesis that glucose and/or insulin regulate α-MSH *in vivo*. Since ACTH is co-localized with α-MSH in human corticotroph cells, we tested whether α-MSH secretion could occur independently of ACTH co-release. We did not find any change in ACTH levels after glucose administration in either lean or obese humans (Figure 3A). To further ascertain whether the levels of α-MSH were augmented by the direct effect of glucose, we compared the levels of α-MSH after ip glucose or saline administration in lean mice. We found a significant peak of α-MSH at 15 min (66.8 pM, $p < 0.01$) after the glucose challenge and no changes after saline injection (Figure 3D). To establish whether this response was due to POMC cell activation, we studied mice with disrupted K_{ATP} channel function in POMC cells (POMC-mutKir6.2 mice) [15]. These mice exhibited no change in α-MSH secretion in response to glucose administration (Figure 3E). Altogether, these results strongly support the hypothesis that pituitary POMC cells are responsible for sensing the plasma glucose fluctuations, which, in turn, stimulates α-MSH secretion.

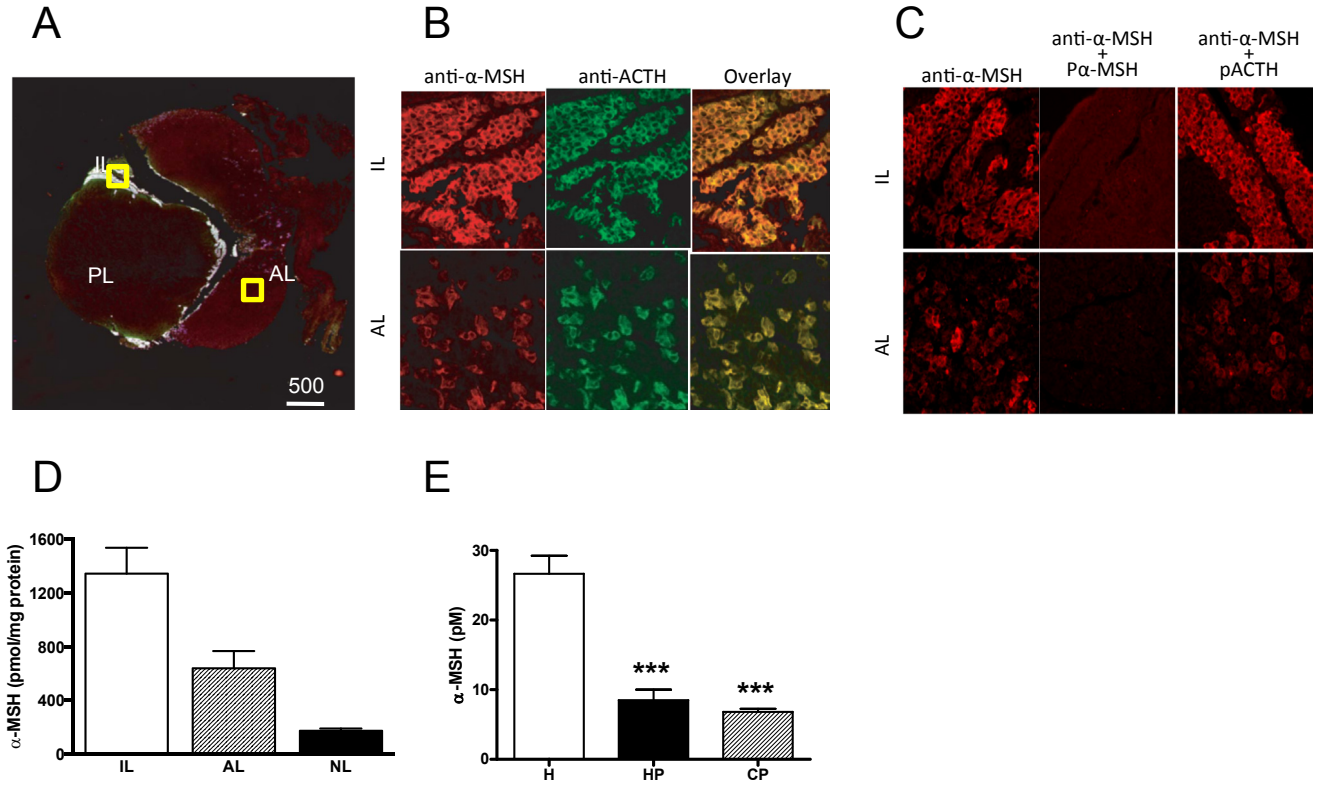

Figure 2: The pituitary is the source of α-MSH, and its secretion is regulated by glucose. A. Representative microphotograph of a Japanese macaque pituitary showing AL: anterior lobe, IL: intermediate lobe, PL: posterior lobe. Samples were taken from areas depicted in yellow B. Confocal digital images (CDI) of double-label immunofluorescence for α-MSH (red) and ACTH (green) expression. C. CDI of single-label immunofluorescence for α-MSH (red). IL has mostly co-localized α-MSH/ACTH expressing cells. The AL contains some co-localized α-MSH/ACTH expressing cells and some cells only expressing ACTH. D. α-MSH concentrations determined by RIA in different areas of the rhesus macaque pituitary ($n = 3$). E. Plasma α-MSH levels in healthy humans (H, $n = 27$), patients with hypopituitarism (HP, $n = 4$), and patients with craniopharyngioma after surgery (CP, $n = 15$), ***$p < 0.001$ vs. healthy controls by one-way ANOVA followed by Bonferroni's Test. Data are expressed as mean ± SEM. See also Figure S1.

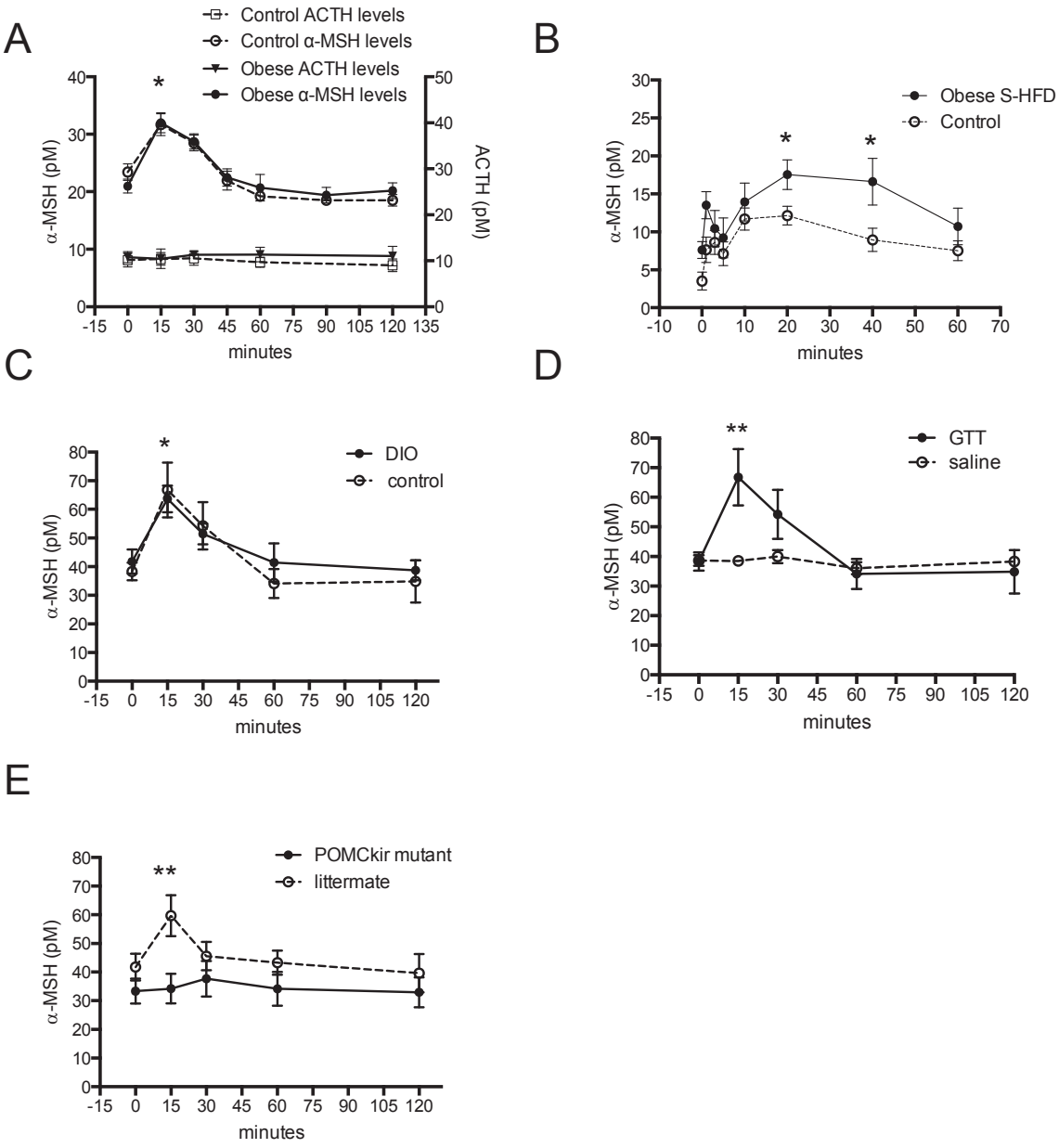

Figure 3: Glucose increases levels of plasma α-MSH, but not ACTH, in humans, monkeys, and mice. A. α-MSH levels and ACTH levels during an OGTT in normal body weight (control) and obese children (n = 6). B. α-MSH levels during an ivGTT in control and obese S-HFD Japanese macaques (n = 5). C. α-MSH levels during an ip GTT in control and DIO mice (n = 6). D. α-MSH levels after ip GTT/saline administration in lean mice (n = 6). E. α-MSH levels during an ip GTT in POMC-Kir6.2 mutant mice and its littermate (n = 10). Results are mean ± SEM. *p < 0.05 and **p < 0.01 by two-way ANOVA. In figures A–C, * represents the significance at time 15 or 20–40 min vs. basal values (time 0). See also Figures S2 and S3.

2.1.3. Systemic α-MSH increases glucose clearance

Next, we probed the role of systemic α-MSH in glucose regulation. To achieve that, we first conducted a short-term systemic α-MSH infusion in lean mice and found that it did not modify glucose levels in fasted condition (Figure S4A). We then monitored glucose excursions during ip GTT's in mice that received either a 3 h saline or α-MSH infusion. We treated lean mice with a series of α-MSH doses ranging from 0.0005 μg/h to 1 μg/h and found a significant improvement in glucose tolerance at a dose of 0.001 μg/h α-MSH, which corresponds to 90 pM of α-MSH in blood (Figure 4A and C). We did not find any further improvement in glucose tolerance using higher doses of α-MSH (Figures 4A and S5A). In separate experiments, using a recently validated technique [16], we confirmed that α-MSH infusion increased whole-body 2-deoxy-D-[1-^{14}C]glucose (2DG) clearance (Figures S4C and D). In spite of enhanced glucose tolerance, the insulin levels were not statistically lower in α-MSH treated animals compared with saline treated mice (Figure S4B), supporting the premise that the main effect of α-MSH was on glucose disposal in skeletal muscle.

To prove this notion, we employed hyperinsulinemic-euglycemic clamp to reveal any tissue-specific regulation of α-MSH on glucose homeostasis (Figure S6A). Of note, body weight, blood glucose

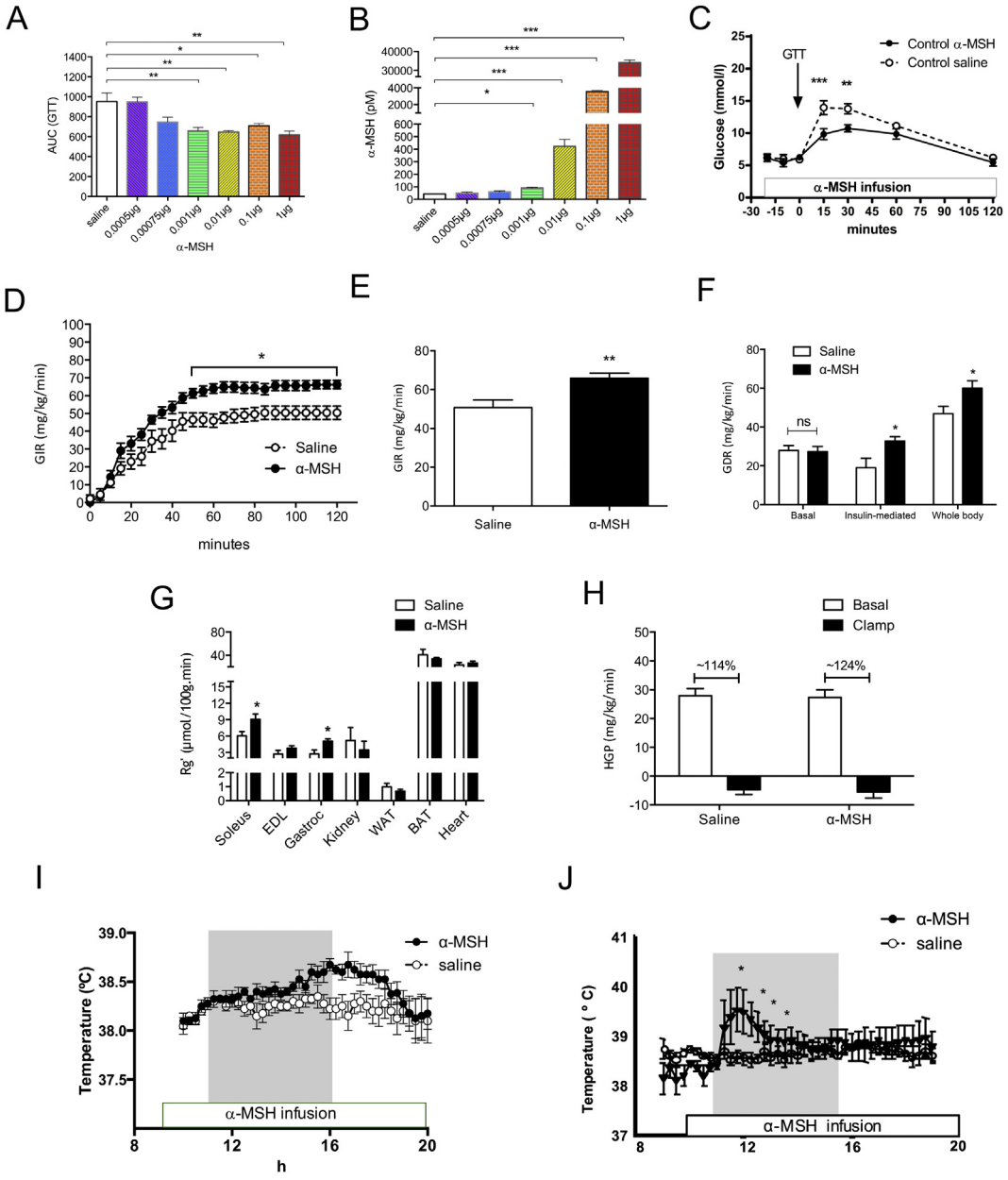

Figure 4: α-MSH infusion in lean mice enhances glucose clearance by increasing muscle glucose uptake *in vivo*. Very low plasma α-MSH level is associated with glucose intolerance. A—B. Area under curve of GTT and plasma α-MSH levels during 3 h saline/α-MSH infusion using different doses of α-MSH (n = 4—14). C. Systemic α-MSH infusion (1 μg/h) increases glucose disposal during ip GTT in lean mice, (**$p < 0.01$, ***$p < 0.001$ vs. saline infusion, n = 6—9). D. α-MSH increases glucose infusion rate in lean mice during a 2 h hyperinsulinemic-euglycemic clamp (n = 7). E. α-MSH increases GIR during steady state. F. Systemic α-MSH increases insulin-mediated and whole body glucose disposal rate without altering basal Rd. G. Under clamp conditions, α-MSH enhances glucose uptake into soleus and gastrocnemius muscle but not into other metabolically active tissues. H. Hepatic glucose production remains unchanged between saline and α-MSH treated group. I. Post-prandial muscle temperature after systemic α-MSH infusion (external jugular vein, 100 μg/h) or saline in sheep. J. Post-prandial muscle temperature after direct α-MSH infusion (1 μg/h) or saline into the femoral artery. A datalogger was surgically inserted into the vastus lateralis muscle of sheep to read temperature at 15′ intervals (n = 4). Grey box represents food availability (11:00 to 16:00 h). $p < 0.01$ by AUC analysis. Data are expressed as mean ± SEM. *$p < 0.05$, **$p < 0.01$ saline vs. α-MSH. See also Figures S4, S5 and S6

concentrations, and insulin levels were equivalent between saline and α-MSH treated mice (Figure S6B—S6D). During the hyperinsulinemic-euglycemic clamp, mice treated with α-MSH required higher glucose infusion rate to maintain normal glucose levels (Figure 4D and E). Interestingly, these mice also displayed a marked increase in insulin-mediated and whole body glucose disposal, which brought forward an additive effect of α-MSH in glucose clearance under clamp condition (Figure 4F). Moreover, increased glucose uptake was significant in skeletal muscles, in particular the soleus and the gastrocnemius muscle as opposed to other metabolically active tissues such as kidney, adipose tissues and heart (Figure 4G). Importantly, endogenous hepatic glucose production (HGP) did not differ between both groups, which revealed a direct action of α-MSH on skeletal muscle (Figure 4H). No further effect of α-MSH on the liver was observed as evidenced by quantitative RT-PCR of gluconeogenic enzymes after clamp or systemic infusion studies (Figure S6E). In addition, we

validated the direct effect of exogenous α-MSH on muscle by using an established model of diet-induced entrainment of a thermogenic response in sheep [17]. We found that systemic α-MSH infusion increased post-prandial muscle temperature in sheep (Figure 4I). Furthermore, α-MSH infusion into the leg femoral artery resulted in an increase in muscle temperature, while we were unable to measure changes on the contra-lateral saline infused site (Figure 4J), further demonstrating a direct effect of α-MSH on skeletal muscle. Together, these data suggest that α-MSH acts directly on skeletal muscle to increase glucose clearance and thermogenesis and this effect is independent of hepatic glucose production.

2.1.4. α-MSH increases glucose uptake in skeletal muscle

To determine if the effect of α-MSH on skeletal muscles was direct, we took an *ex vivo* and *in vitro* approach. During these studies, it became evident that α-MSH increased basal glucose disposal in a dose-responsive manner (Figure S7). Furthermore, data from *ex vivo* 2-DG uptake of isolated soleus displayed an enhancement of 2-DG uptake induced by α-MSH on top of insulin-mediated 2-DG uptake (Figure 5A). Similar results were observed in cultured myotubes (GLUT4myc-L6) (Figure 5B). Using the cultured myotubes, we also measured the oxygen consumption rate (OCR) and the extracellular acidification rate (ECAR, assessing glycolysis) applying an extracellular flux analyzer system (Seahorse®). We detected a dose-dependent increase of glycolysis induced by α-MSH (Figure 5C), without a concomitant change in OCR (data not shown), indicating that the main short-term action of α-MSH is through glycolysis and not increased mitochondrial respiration. Interestingly, we also found that culturing L6 myotubes in high concentrations of glucose (25 mM) blocked α-MSH induced glycolysis (Figure S7). To this end, these results are in agreement with the concept that α-MSH acts directly on skeletal muscles to regulate glucose homeostasis.

2.1.5. MC5R is crucial for peripheral α-MSH action in muscle

To ensure that the effect observed was not confounded by any possible actions in the CNS, we repeated the α-MSH infusion after blocking brain melanocortin receptors (MC3/MC4R) with icv injection of their endogenous antagonist, AgRP. We established a dose of AgRP (1.0 nmol) that completely abolished the anorectic effect of MTII (Figure S10A), thereby demonstrating complete blockade of the MC3/MC4R. We found that this blockade did not prevent the α-MSH mediated improvements in glucose tolerance (Figure 6A). In a separate experiment, we corroborated the role of peripheral α-MSH on glucose homeostasis by administering lean mice with neutralizing antibodies against α-MSH through the tail vein (iv) or the lateral ventricle (icv). Lean mice were rendered glucose intolerant when neutralizing antibodies against α-MSH were given systemically as opposed to icv antibody treatment (Figure S10B). This is supported by a significant increase in blood glucose levels during a GTT compared to mice that received purified rabbit IgG as control (Figure 6B). Notably, the antibodies did not impact basal glycemia (antibody treated: 8.5 ± 1.3 vs saline treated: 8.6 ± 1.6 mmol/l, respectively). Strikingly, POMC-mutKir6.2 mice (with no change in α-MSH secretion in response to glucose administration) were found to be glucose intolerant (Figures S9A and B), supporting the premise that α-MSH from the pituitary acts upon skeletal muscle to regulate glucose homeostasis in response to glucose load. To mechanistically delineate the action of α-MSH on skeletal muscle, we first assessed which melanocortin receptor (MCR) subtypes were expressed in skeletal muscle. Out of all the different subtypes of melanocortin receptors, we found that only MC5R was highly expressed in skeletal muscles of both lean and DIO mice (Figures 6C and D and S10C, S10D). Going further, we investigated whether MC5R mediates the action of α-MSH by using PG-901, which is a human and mouse MC5R specific agonist and a neutral antagonist of human and mouse MC3/4R [18,19]. Short-term incubation of PG-901 increased glucose uptake in GLUT4myc-L6 myotubes (Figure S11). Following that, we performed similar *in vivo* infusion and GTT studies to assess glucose disposal in mice lacking MC5R (MC5R KO) [20]. As shown in Figure 6E, there were no differences in glucose tolerance between α-MSH and saline infused MC5R KO mice. On the contrary, glucose tolerance was significantly enhanced by α-MSH infusion in wild-type littermates. In addition, α-MSH-mediated glucose disposal was completely abrogated in the isolated skeletal muscle of MC5R KO mice (Figure 6F). Furthermore, lean mice given highly selective MC5R antagonist [21] ip displayed significantly higher glucose levels relative to the saline group (Figure 6G). Interestingly, MC5R KO mice showed hyperinsulinemia when fasted and 30 min after glucose administration (Figure 6H), suggesting that MC5R KO mice compensate for the lack of α-MSH with an increase of insulin to restore euglycemia. These results illustrated that MC5R plays a vital role in mediating glucose clearance in skeletal muscle upon binding to α-MSH.

2.1.6. A combined therapy of nonselective/selective phosphodiesterase 4 inhibitor and α-MSH ameliorates glucose intolerance in obese mice

In healthy individuals, blood glucose is tightly regulated; however, a prominent feature of diet-induced obesity is glucose dysregulation and the eventual development of type 2 diabetes. Therefore, to examine the therapeutic relevance of α-MSH-mediated glucose disposal, we next probed the effect of α-MSH in mice fed with HFD. Intriguingly, we did not find any improvement in glucose tolerance in DIO mice (Figure 7A). In line with the *in vivo* finding, neither α-MSH nor insulin increased glucose disposal in isolated soleus muscle obtained from DIO mice, which highlighted an insulin resistant and possibly a α-MSH resistant phenotype in these mice (Figure 7B). Since melanocortin receptors are members of 7-transmembrance G protein-coupled receptor (GPCR), MC5R couples to stimulatory G protein alpha upon ligand binding, which classically increases cyclic adenosine monophosphate (cAMP) production and PKA activity [22]. We next measured cAMP levels in the soleus muscle of lean and DIO mice that received α-MSH infusion during a glucose challenge. We found that cAMP levels were significantly elevated in lean mice in contrast with DIO mice where the effect was abrogated (Figure 7C). In addition, selective inhibition of PKA by H89 in L6 cells revealed that the activation of PKA was necessary for α-MSH-mediated glucose uptake (Figure 7D).

Further, we measured phosphodiesterase (PDE) protein levels in muscles from lean and DIO mice to inquire whether the failure of α-MSH to induce glucose uptake in obesity was associated with the inability to increase cAMP. Interestingly, we found a higher expression of PDE4B in obese compared to lean mice (Figure 7E and F). Based on this result, we next isolated soleus muscles from DIO mice and performed an *ex vivo* incubation with theophylline, a non-selective PDE inhibitor, together with α-MSH. The inhibition of PDEs in the presence of α-MSH was able to restore glucose uptake in muscles from DIO mice (Figure 7G). To test the physiological relevance of combined PDE inhibition and α-MSH *in vivo*, we pretreated mice with theophylline for 5 days prior to α-MSH infusion. Of note, theophylline treatment did not modify basal glucose levels, but it significantly improved glucose tolerance in obese mice (AUC $p < 0.01$) (Figure 7H). We also pretreated mice with rolipram, which selectively inhibits PDE4, particularly the PDE4B isoform [23]. Rolipram pretreatment for 5 days prior to α-

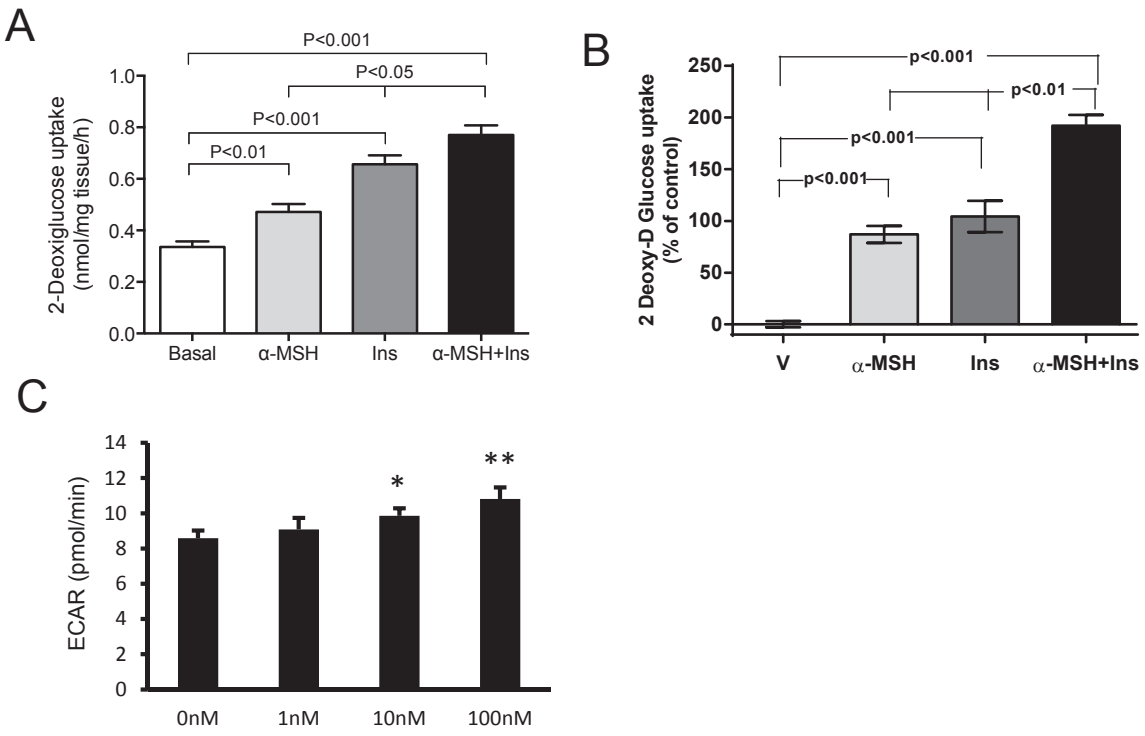

Figure 5: α-MSH increases glucose uptake and glycolysis in *ex vivo* skeletal muscle and differentiated L6-cells. A. α-MSH increases glucose uptake in soleus muscles from control mice (n = 8). Muscles were incubated with Insulin 10 nM, α-MSH 100 nM for 20′. Radioactivity was measured in muscle lysates by liquid scintillation counting. B. α-MSH increases glucose uptake in differentiated L6-cells and potentiate insulin action. Each bar represents an average from 3 independent experiments, n = 3 in each one. Cells were preincubated with α-MSH for 1 h before starting the glucose uptake. Radiolabeled 2-deoxy-D-[2,6-^{3}H]glucose (1 mmol/l, 0.5 μCi/ml), 10 nM insulin, 100 nM α-MSH or both was added to the corresponding well and maintained for 15′. C. Glycolysis time-course (as extracellular acidification rate; ECAR) was measured by Seahorse analyzer from α-MSH (1–100 nM, *p < 0.05 and **p < 0.01 vs. basal). Data are expressed as mean ± SEM. See also Figures S7 and S8

MSH infusion significantly improved glucose disposal during GTT in obese mice (AUC p < 0.05) (Figure 7I). Surprisingly, we did not find an improvement in glucose tolerance in DIO mice with either theophylline or rolipram alone (Figure 7H and I). Hence, this suggests that sub-chronic treatment of phosphodiesterases alone is not sufficient to reverse glucose intolerance; however, it is able to potentiate α-MSH-mediated glucose disposal to restore glucose tolerance in DIO mice. Collectively, our results strongly support a novel model where peripheral α-MSH regulates glucose homeostasis by acting via MC5R-cAMP-PKA pathways in skeletal muscle.

3. DISCUSSION

3.1. Feeding and glucose increase α-MSH secretion

These studies describe a new endocrine circuit that is capable of modulating post-prandial glucose homeostasis. Our studies showed that α-MSH levels have a prandial pattern of secretion increasing after meal consumption. Furthermore, α-MSH peaks occurred after consumption of a HCD, suggesting that diet composition influences the physiological release of α-MSH. We observed in humans, non-human primates, and mice that α-MSH levels consistently increased in response to plasma glucose excursions, suggesting glucose is a regulator of plasma α-MSH. In accordance with the presence of glucose-sensing cells within the pituitary AL [5], we found an increase in α-MSH release from isolated pituitaries incubated with glucose. Moreover, mice lacking pituitary glucose-sensing capacity (POMC mutKir6.2) [15] displayed glucose intolerance, which further substantiates the hypothesis that the pituitary senses and reacts to changes in glucose homeostasis. This could be explained in part by the large reduction (~70%) in plasma α-MSH levels in HP and CP patients. These findings also demonstrate that the pituitary melanocortin-secreting cells utilize a beta-cell-like mechanism to couple extracellular glucose levels to hormone secretion. Importantly, the activity of the HPA axis did not change during a GTT, as was previously demonstrated [24], suggesting that the increase in α-MSH secretion is a specific effect of glucose-mediated processing/secretion of α-MSH from pituitary cells.

3.2. Circulating α-MSH is secreted from the pituitary

There is a preponderance of data supporting the production of α-MSH by pituitary cells and extrapituitary cells, such as keratinocytes, monocytes, astrocytes, gastrointestinal and the brain [25]. Here, we showed that a substantial amount of α-MSH in the blood (~70%) was produced by the pituitary in higher mammals. This finding was demonstrated by *in vitro* studies determining α-MSH secretion from dissected areas of the pituitary and by measuring α-MSH levels in patients with normal, low- or non-functioning pituitaries.

While in rodents the IL is anatomically well-defined, in adult humans and non-human primates, it is a rudimentary structure along the border of the anterior and neural lobes consisting of a small number of POMC-synthesizing cells [26,27]. In line with other reports, we showed that AL and IL cells are capable of producing α-MSH in human and non-human primate adult pituitary [3,28,29]. In addition, patients with acute phase septic shock or untreated Addison disease displayed elevated α-MSH levels [30,31].

POMC-derived peptides such as ACTH, as well as α-, β-, and γ-MSH, exert their pleiotropic effects via binding to MCRs at different binding affinity and potency. In the present study, we focus exclusively on the

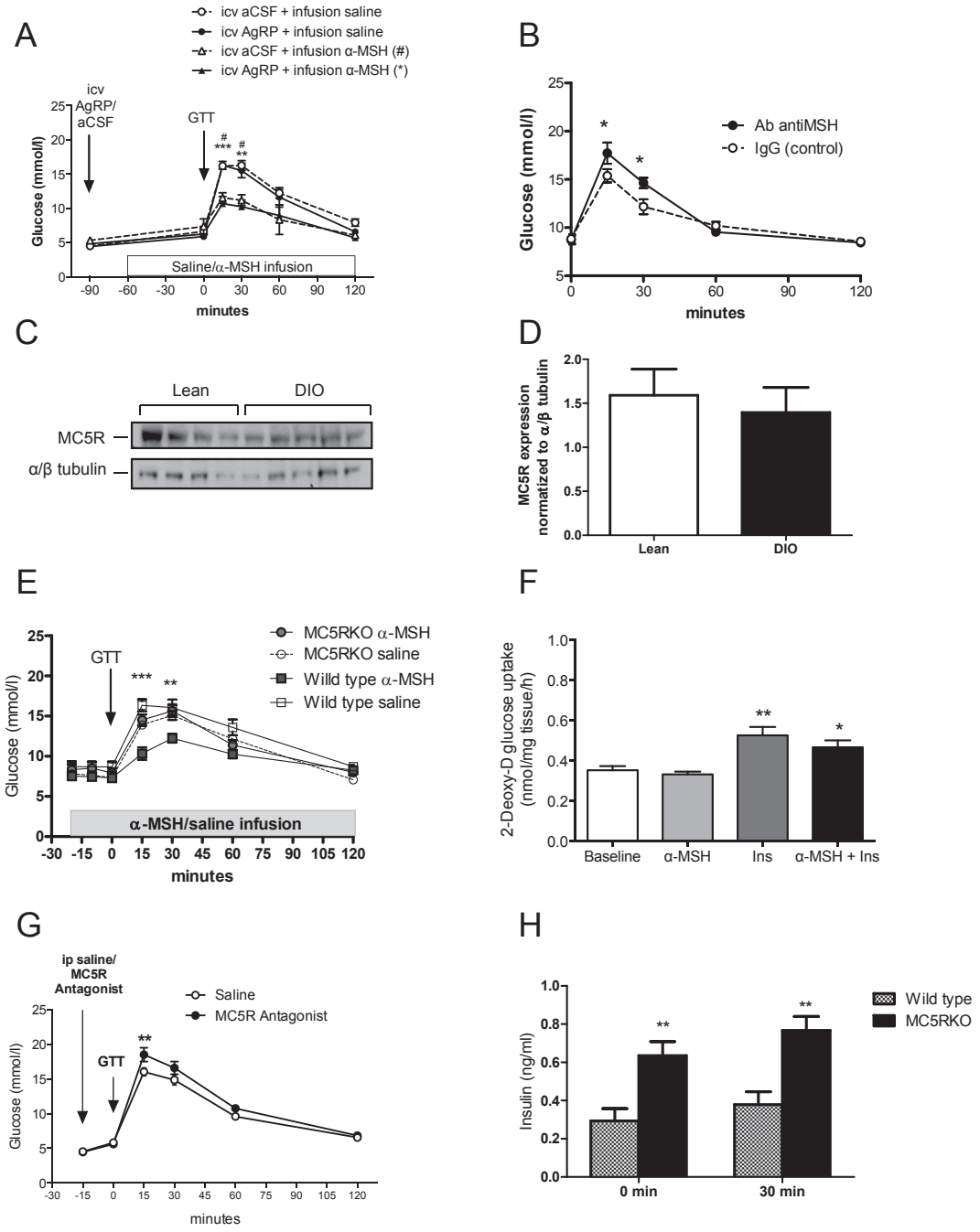

Figure 6: Peripheral α-MSH acts via the MC5R to increase glucose disposal *in vivo*. A. Blockade of MC3/MC4R with icv AgRP (1.0 nmol, 1 μl) prior to α-MSH infusion cannot prevent the increase of glucose disposal during GTT (n = 4) (#$p < 0.05$ vs. icv aCSF + infusion α-MSH, **$p < 0.01$, ***$p < 0.001$ vs. icv AgRP + infusion α-MSH). The dose AgRP was selected from a cumulative food intake experiment (Figure S4E). B. Neutralizing α-MSH IgG reduces glucose disposal during a GTT (*$p < 0.05$ and **$p < 0.01$ vs. IgG control). Mice received an iv injection of anti α-MSH (20 μg/ml) or rabbit IgG (n = 9). GTT was performed 90′ after injection. C. MC5R expression was not different in soleus muscles from lean and DIO mice (n = 4–5). D. Quantification of MC5R measured by Western blot as a ratio of α/β tubulin. E. Systemic α-MSH infusion does not increases glucose disposal during ip GTT in MC5R KO mice (n = 6–14). *$p < 0.01$ and ***$p < 0.001$ by two-way ANOVA followed by Bonferroni's Test for each group vs littermate α-MSH infusion group. F. α-MSH does not increase glucose uptake in soleus muscles from MC5R KO mice (n = 5). *$p < 0.05$, **$p < 0.01$ vs. baseline by one-way ANOVA followed by Bonferroni's Test. G. Lean mice given ip MC5R antagonist (4 nM) display higher glucose levels during a ip GTT (**$p < 0.01$ vs. saline, n = 8). MC5R antagonist was given 15′ before glucose challenge. H. MC5R KO mice show higher level of insulin at baseline state and after a 30′ glucose challenge (ip GTT, 1 mg/g, n = 6). Data are expressed as mean ± SEM. **$p < 0.01$ by two-way ANOVA followed by Bonferroni's Test. See also Figures S9, S10 and S11

role of α-MSH on glucose homeostasis using a highly specific radioimmunoassay plasma α-MSH that was previously described [32,33]. Noteworthy, the assay has no cross-reactivity with ACTH and β-, and γ-MSH (by standard displacement curve) so the α-MSH detected in this study is not a degradation product of ACTH [32]; α-MSH has an identical amino acid sequence to the residues of ACTH (1—13) and α-MSH levels overlap with ACTH levels. Consistent with the literature, we found that ACTH levels were not altered following overnight fasting [34]

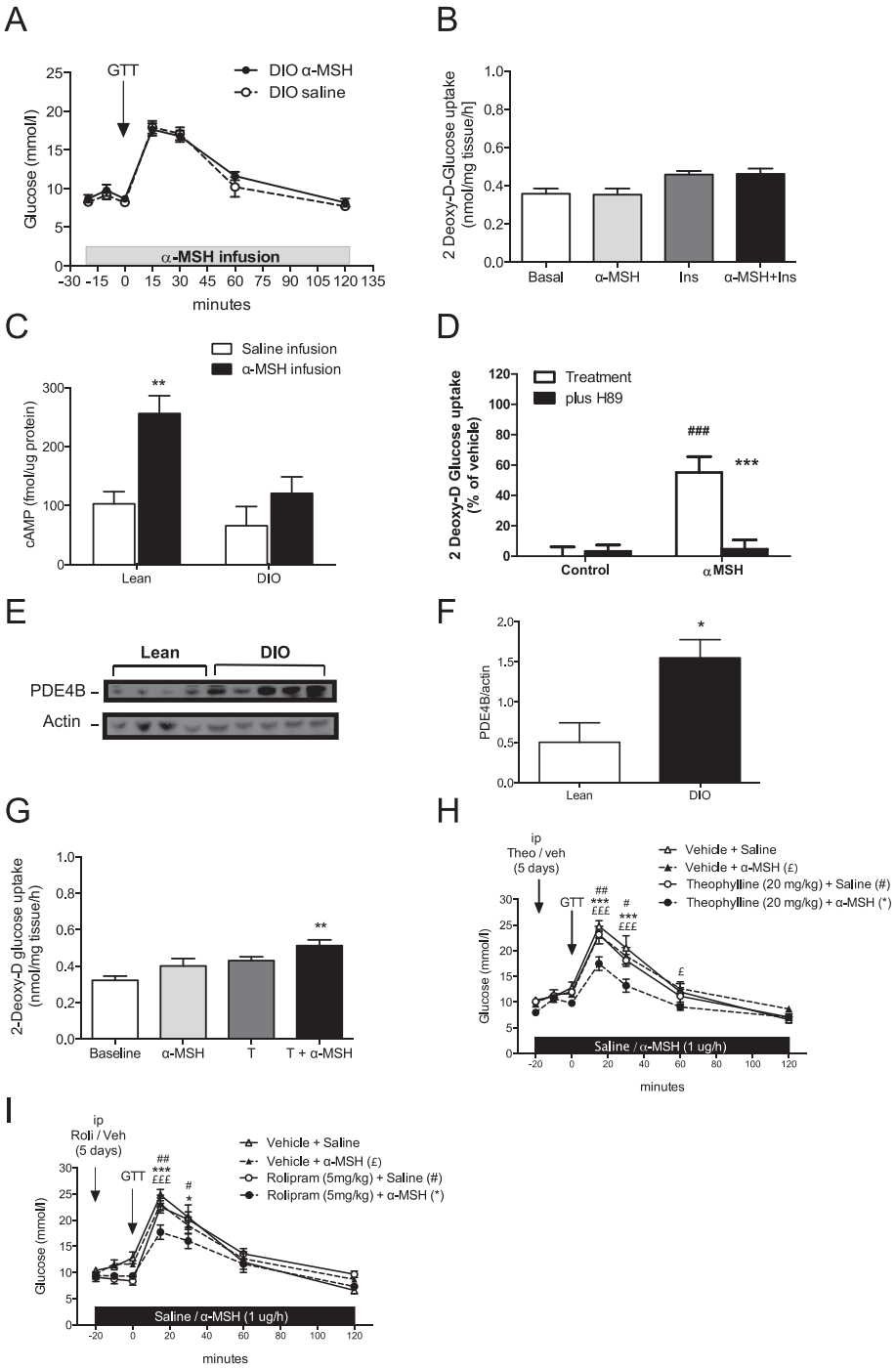

Figure 7: Inhibition of PDE's enhances the effect α-MSH on glucose disposal in DIO mice. A. Systemic α-MSH infusion did not increase glucose disposal in DIO mice (n = 8). B. Insulin and α-MSH-mediated glucose uptake was abrogated in *ex vivo* soleus extracted from DIO mice (n = 5). C. Systemic α-MSH infusion (1 μg/h) increases cAMP levels in muscles of lean mice instead of DIO mice (n = 5–7). cAMP concentration was measured after 45'of initiating α-MSH infusion and 25′ of starting GTT. D. α-MSH (100 nM) increases glucose uptake in differentiated L6-cells, and it is inhibited by pretreatment with a selective inhibitor of cAMP dependent protein kinase (15 μM H89 during 30′). ##p < 0.01 vs control, ***p < 0.001 vs H89. E. PDE4B expression in soleus muscle was higher in DIO mice than lean mice in basal conditions (n = 4–5). F. Quantification of PDE4B measured by Western blot as a ratio of β–actin (*p < 0.05 vs. lean). G. α-MSH (100 nM) increases glucose uptake in soleus muscles from DIO mice after a preincubation with a non-selective PDE inhibitor (Theophylline; 100 uM) for 20'. **p < 0.01 vs. basal baseline by one-way ANOVA followed by Bonferroni's Test. H. Pre-treatment with daily ip theophylline (20 mg/kg) for 5 days before systemic α-MSH infusion (1 μg/h) increases glucose disposal during ip GTT in DIO mice (n = 7). As a control, mice were pre-treated with the correspondent vehicle (DMSO 50%). ***p < 0.001 vs. Theophylline + α-MSH, £p < 0.05 and £££p < 0.001 vs. vehicle + α-MSH, #p < 0.05 and ##p < 0.01 vs. theophylline + saline by two-way ANOVA followed by Bonferroni's Test. I. Pre-treatment with ip Rolipram (5 mg/kg) two times daily for a period of 5 days before systemic α-MSH infusion (1 μg/h) increases glucose disposal during ip GTT in DIO mice (n = 8–9). It was compared to DIO mice receiving saline infusion. The systemic α-MSH infusion and posterior GTT was exactly as described in Figure 4. Data are expressed as mean ± SEM. *p < 0.05 and ***p < 0.001 vs. rolipram + α-MSH, £££p < 0.001 vs. vehicle + α-MSH, #p < 0.05 and ##p < 0.01 vs. rolipram + saline by two-way ANOVA followed by Bonferroni's Test.

and during OGTT in humans [35,36]. Thus the peptides described as α-MSH here are specifically α-MSH levels.

3.3. Physiological levels of α-MSH increase glucose tolerance and muscle glucose uptake

The indication that peripheral α-MSH has a role in glucose homeostasis came from the finding that the infusion of α-MSH increases glucose tolerance during a GTT in lean mice. Importantly, these results were obtained using doses of α-MSH within the physiological range. Moreover, this effect was specific to α-MSH as mice display reduced glucose tolerance during GTT after systemic administration of α-MSH neutralizing antibody. Studies have documented that central activation of MCRs play a role in skeletal muscle glucose uptake [37,38]. Contrary to our results, blockade of brain MC3/MC4R could not prevent the increase in glucose tolerance after a glucose challenge during α-MSH infusion. In fact, the response observed in mice was partly at a cellular level given that α-MSH stimulated glucose uptake in soleus and gastrocnemius muscle biopsies extracted from lean mice in our *ex vivo* studies. Further, during hyperinsulinemic-euglycemic clamp, we showed that the addition of α-MSH enhanced glucose clearance through soleus and gastrocnemius muscles without altering hepatic glucose production and gluconeogenic enzymes expression in the process, further bolstering the action of α-MSH on skeletal muscle. To our knowledge, this is the first evidence of the direct action of α-MSH on skeletal muscle to regulate glucose homeostasis.

While insulin is the principal regulator of glucose homeostasis, we believe that pituitary α-MSH plays a modulatory role in postprandial regulation of blood glucose, but is not a substitute for insulin. Interestingly, POMC homozygous null mice showed a normal response to GTT [39] and, recently, a rare case of human with complete POMC deficiency and type 1 diabetes was described; the patient had insulin requirements appropriate for his age and pubertal development [40]. It seems that the lack of POMC (α-MSH) in both models is not enough to modify the glucose homeostasis. In contrast, we found that POMC-mutKir6.2 mice had very low plasma α-MSH levels and were unable to increase α-MSH secretion in response to glucose administration. In addition, POMC-mutKir6.2 mice are glucose intolerant, which highlights the importance of α-MSH in the regulation of glucose homeostasis. Moreover, the fact that MC5R KO mice, which are not obese, require a higher level of insulin to maintain a normal glucose homeostasis support the idea that α-MSH integrates a complementary endocrine circuit that regulates postprandial glucose homeostasis, mainly through the increases muscle glucose intake via a different pathway to insulin. Data regarding the potential correlation of plasma α-MSH with insulin resistance/obesity is conflicting. While some studies showed that plasma α-MSH levels correlated with insulin resistance/obesity in humans [10,11], others claimed that these were unrelated to body composition [31,41]. Our results are in agreement with the latter, as we did not observe any relationship between plasma α-MSH levels and body weight or HOMA (an index of insulin resistance) in any of the species analyzed.

Several studies have addressed the role of circulating α-MSH in the regulation of energy homeostasis [9,42,43] mainly focusing on fat metabolism and thermal regulation [42] but not on glucose regulation. Intriguingly, An et al. showed that α-MSH enhances glucose uptake stimulated by insulin in the C2Cl2 mouse muscle cell line. However, data regarding the effect of α-MSH alone on glucose uptake are lacking in this study [6]. Further, we showed that α-MSH increases glycolysis in L6 muscle cells and induces anaerobic respiration to produce ATP and lactic acid. Moreover, the increase in muscle temperature of the sheep suggests a local and direct action of α-MSH on femoral muscle after α-MSH artery infusion. Altogether these results indicate that α-MSH induces energy consumption in the muscle.

In addition, the extracellular flux data indicate incomplete glucose oxidation, and this may explain why the effect is only seen in glycolytic muscle (Gastrocnemius vs. soleus muscle). Of note, our data do not exclude glycogen production in muscle. We did not find any changes in mitochondrial respiration and FAO in L6 cells incubated with α-MSH as described by An et al. in both C2C12 myotubes and primary muscle cells [6], Instead, we found a dose—response increase in glycolysis after incubation with α-MSH. The discrepancy could be due to the use of different cell lines to determine FAO and the methodology employed in this study. However, we cannot exclude the increase in FAO in response to α-MSH infusion *in vivo*.

3.4. MC5 R and cAMP mediate the action of α-MSH on glucose tolerance and muscle glucose uptake

Five MCR subtypes have been described [2,22]. We confirmed that only MC5R was highly expressed in skeletal muscle [44]. This receptor has been previously implicated in water repulsion, pheromone secretion, and regulation of several exocrine glands [20,45]. Interestingly, a recent human study showed that single-nucleotide polymorphism in the MC5R was associated with type 2 diabetes in obese subjects [46]. MC5R is ubiquitously expressed in peripheral tissues, and it is similar to the MC1R and MC4R in its capacity to recognize α-MSH and ACTH but not γ-MSH (β-MSH is not produced in rodents). Thus, it is possible that other melanocortins besides α-MSH can participate in the mechanisms described above. However, neither their physiological relevance nor their postprandial secretion patterns is known.

MC4R has been extensively studied, and it has a critical role in the central control of metabolism. However, our studies ruled out a role for central melanocortins using CNS blockade of melanocortin receptors and using MC5R agonist PG-901 as an antagonist at MC4R. It has also been demonstrated that genetic background has a modifying effect on the phenotype of MC4R KO mice. The MC3R has a clear metabolic phenotype, and this manuscript describes an important role of MC5R in modulation of glucose homeostasis in muscle [47—49]. Therefore, the role of peripheral melanocortin system in regulating glucose metabolism should receive more attention and further investigation.

In our *ex vivo* and *in vivo* studies presented here, the effect of glucose uptake or glucose disposal driven by α-MSH was completed blunted in MC5R KO mice. Additionally, we showed that specific inhibition using MC5R selective antagonist caused a similar reduction in glucose tolerance in lean mice to that of α-MSH neutralizing antibody, suggesting that MC5R is essential to mediate the action of α-MSH in the periphery. This finding also put forward a tonic role of α-MSH on MC5R during basal condition as blockade of MC5R results in hyperglycemia during GTT in these mice. Collectively, these results corroborated the crucial role of MC5R in regulating glucose homeostasis.

MCRs couple to stimulatory G protein to increase cAMP production in response to receptor activation. However, activation also involves several other cAMP independent pathways [50]. We found that α-MSH increases cAMP levels in the muscle of lean mice during GTT. Most of the published studies showed that an increase of cAMP subsequently enhances the activity of PKA. However, it has been recently demonstrated that cAMP can mediate glucose uptake in smooth muscle independently of PKA activation [51]. We discovered that the activation of PKA is necessary for α-MSH mediating glucose uptake because pre-

incubation of L6 muscle cells with a potent selective PKA inhibitor (H89) abolished the effect of α-MSH. In our recent study, Møller et al. reported that α-MSH stimulated phosphorylation of short isoform of TBC1D1 but not TBC1D4 (also called AS160) in soleus muscle (PLoS One, in press); two related Rab-GTPase activating proteins that are involved in the translocation of GLUTs in response to insulin/exercise [52]. GLUT12 seems to be a likely candidate to be responsible for α-MSH-mediated glucose uptake as it accounts for 12% of insulin-induced glucose transporters translocation in humans muscles [53]. However, additional studies are required to identify which glucose transporter is involved as Møller et al. did not observe a change in GLUT4 translocation upon α-MSH stimulation in cultured myocytes (PLoS One, in press).

3.5. Blockade of phosphodiesterases restores α-MSH mediated glucose uptake to muscle from obese mice

Throughout this study, α-MSH has consistently failed to produce any effect associated with glucose homeostasis under obese/hyperglycemic conditions. Indeed, α-MSH did not modify the glucose tolerance during GTT in obese mice, did not increase glucose uptake in isolated muscles from DIO mice, and did not drive glycolysis in cells cultured in high glucose.

The fact that MC5R expression was similar in lean and DIO mice suggests that the failure of α-MSH to induce glucose uptake in hyperglycemic subjects was not due to the lack of receptor. In addition, cAMP levels in the muscle of obese mice were unaltered after α-MSH treatment indicating the failure of signal transduction. Furthermore, PDE expression was higher in the muscle of DIO mice, suggesting that the blunted response in cAMP activation in DIO mice could be due PDEs inactivating cAMP [54].

Interestingly, by blocking PDE activity with theophylline, a non-selective PDEs inhibitor, we were able to restore α-MSH-mediated glucose uptake in isolated muscles from obese mice. More importantly, we found that both selective and non-selective PDE4B inhibition with rolipram and theophylline, respectively, were able to enhance the effect of α-MSH infusion and significantly improve the glucose tolerance during GTT in obese mice. Restoration of this mechanism in the obese could potentially open new avenues to adjunctive pharmacological treatments to reduce postprandial glucose excursions. It was recently shown that another PDE4 inhibitor roflumilast reduced glycosylated hemoglobin and post-meal glucose in a trial in type 2 diabetics [55], although the mechanism of the effect was not determined. Our work suggests that PDE4 inhibitors should be further investigated in type 2 diabetes and perhaps in combination with α-MSH.

3.6. Limitations

The fact that the MC5R KO mice are not diabetic seems to question the role of MC5R in glucose metabolism. Although they appear metabolically normal, MC5R KO mice are hyperinsulinemic at baseline state and after a glucose load. These mice required twice the level of insulin relative to their wildtype littermates at baseline and at the peak of a GTT to maintain a normal glucose tolerance, suggesting an increase in insulin secretion to compensate for a lack of α-MSH action via MC5R on muscle. The phenomenon of compensation in KO mice is not unusual. For example, despite the strong pharmacological evidence supporting the role of NPY and AgRP in energy balance a conventional knockout of either NPY or AGRP results in normal body weight, adiposity, and food intake. On the contrary, postnatal genetic ablation of AgRP neurons leads to hypophagia and starvation [56]. These observations further demonstrate that there are inherent limitations in approaches using mice that develop while either lacking or over-expressing key proteins of interest.

In conclusion, we have discovered a novel endocrine circuit that regulates postprandial glucose homeostasis. These results demonstrate that in humans, non-human primates, and mice, the pituitary detects circulating glucose and responds with increased α-MSH secretion. Overall, this is the first report showing that the increase in plasma α-MSH exclusively enhances muscle glucose uptake through the direct activation of canonical MC5R-PKA pathways in muscle of lean but not obese subjects; inhibition of phosphodiesterase restores α-MSH mediated glucose tolerance in obese mice. Our discovery provides the basis for future studies to determine how melanocortin control of muscle glucose uptake and glycolysis can be utilized in treating patients with obesity and type 2 diabetes.

4. EXPERIMENTAL PROCEDURES

4.1. Subjects and patients

Twenty-seven normal weight children (15 girls/12 boys, mean age 10 y) and 39 obese children (20 girls/19 boys, mean age 11 y) were studied. In a subgroup of obese (otherwise healthy) and normal weight children (n = 6/per group) an oral GTT (1.75 g/kg, max. 75 g) was performed. α-MSH, insulin and glucose were determined at time points (0′, 15′, 30′, 60′ and 120′). Inclusion criteria were normal weight or obese male or female children age 6–16 years old. Exclusion criteria were current endocrine disorders or intake of prescription medications. In addition, fifteen patients with craniopharyngioma (CP) (mean age 13.8 y) and 4 Hypopituitarism (HP) patients were studied. In most CP patients, hypothalamic involvement, assessed by intraoperative microscopic inspection and/or imaging, was present. Three quarters of patients received percutaneous cranial irradiation because of incomplete resection.

4.2. Hypopituitarism patients

Two patients had no lesion as shown by MRI and presented with GH and TSH deficiency and GH, TSH, and ACTH deficiency, respectively. The other two patients had panhypopituitarism secondary to craniopharyngioma treatment and presented both with combined GH, ACTH, gonadotropin, and TSH and ADH deficiency.

4.3. Monkey model and experiments

For spontaneous secretion of α-MSH: Eight male rhesus macaques 10–18 years-old were studied in an environment controlled for humidity, temperature, and lighting (7:00 am–7:00 pm) at the Oregon National Primate Research Center (ONPRC). Animals were fed 12 biscuits (control monkey diet) (#5047, jumbo size; Purina) at 9:00 am and again at 3:00 pm. Biscuits had an energy density of 3.11 kcal/g (25% protein, 5% fat and 57.5% CH). Monkeys were catheterized as described previously [57] for remote collection of blood samples (hourly during 24 h) and placed in on a control diet or fasted for 24 h. In a subsequent study, blood sampling was performed either at baseline (3:00 pm after a morning fast) or at 8:00 pm after *ad libitum* consumption of control diet (n = 6), High caloric diet (HCD, n = 6), or fasting (n = 6). A HCD consisting of semi-solid cubes weighing ~60 g with an energy density of 3.9 kcal/g (20% protein, 35% fat, and 45% carbohydrate) was provided as noted during specific experiments. Drinking water was continuously available via pressurized drinking spouts.

For ivGTT we studied a model of obese Japanese macaque monkeys that was described in detail elsewhere [58]. Age and weight-matched young adult female Japanese macaque (ages 5–7 y and weight 7–

9 kg) were placed on either a standard monkey chow that provide 14% calories from fat (Monkey Diet # 5052; Lab Diet) or a HFD that supplied 32% calories from fat plus calorically dense treats (Custom Diet 5A1F; Test Diet) and followed over 3 years. During the 3rd year of HFD, five of nine monkeys showed a significant increase in body weight (sensitive to HFD) while the other 4 had normal weights (resistant to HFD). Monkeys were tested after an overnight fast. Glucose (0.6 g/kg; 50% dextrose solution) was administered by continuous infusion over 1 min via the small saphenous vein. Blood samples were obtained before and after infusion via the femoral artery (1, 3, 5, 10, 20, 40 and 60 min). Glucose was measured using an OneTouch Ultra Blood Glucose Monitor (LifeScan).

Three pituitaries were dissected under microscopy to obtain AL and IL. Tissues sections were collected in 2N acetic acid and processed to measured α-MSH content as previously published [33].

4.4. Immunohistochemistry

Four Japanese macaques were fixative perfused in 4% buffered paraformaldehyde and the pituitary harvested and paraffin embedded. Pituitary was cut at 5 μm. Standard IHC methods were used. Detail for this method is provided in the Supplementary methods.

Monkey procedures were performed in accordance with the guidelines and approval of the Oregon National Primate Research Center's Institutional Animal Care and Use Committee.

4.5. Mouse models and experiments

At 5—6 wk of age, C57BL/6J mice (Monash Animal Services) were fed a regular rodent diet (Specialty Feeds) or a HFD (SF04-001; Specialty Feeds) for 20 wk, as previously described [33]. POMC-mutKIR6.2 and MC5R KO mice and their respective wildtype littermates were fed a regular diet for 15—20 wk. Mice were housed (5/cage) in a controlled environment, but they were individually caged during each experiment. Food and water were available *ad libitum*. Body weights were measured weekly. All procedures were performed in accordance with the guidelines and approval of the Monash University Animal Ethics Committee.

4.6. Glucose tolerance test and insulin tolerance test

Glucose tolerance test (GTT) and insulin tolerance test (ITT) were performed as previously described [33]. For GTT, blood samples were obtained after 4 h fast, at 0, 15, 30, 60 and 120 min post glucose challenge. For MC5R KO mice, blood samples (~50 μl) were collected from the saphenous vein at 0 and 30 min after a glucose challenge for the measurement of insulin.

4.7. α-MSH infusion

Mice were instrumented with an arterial catheter (carotid artery) to monitor blood pressure and for sample collection. At the same time, a venous catheter (jugular vein) was placed to infuse α-MSH. The doses infused were 0.0005, 0.00075, 0.001, 0.01, 0.1, and 1 μg/h for 3 h. Blood glucose was measured before and at 10′ and 20′ of α-MSH infusion. After that, mice received an ip glucose injection (GTT, 1 mg/g). Blood glucose levels were measured at 15′, 30′, 60′ and 120 min after glucose challenge. Some mice were sacrificed at time 45 min to perform studies in skeletal muscle, liver and blood.

4.8. α-MSH infusion with pre-treatment of theophylline

Mice were instrumented with a venous catheter and received daily ip injection of theophylline (20 mg/kg) for 5 days or vehicle (DMSO 50%). Then α-MSH (1 μg/h) was infused and GTT performed as above.

4.9. α-MSH infusion with pre-treatment of rolipram

Mice received ip Rolipram (5 mg/kg) or vehicle (DMSO 5%) two times daily for a period of 5 days. Then α-MSH (1 μg/h) was infused and GTT performed as above.

4.10. Hyperinsulinemic—euglycemic clamp

Mice were subjected to jugular vein catheterization 5 days prior to hyperinsulinemic euglycemic clamp studies. Mice were anesthetized with isoflurane (2—3% in oxygen) while an indwelling silastic catheter was inserted into the right internal jugular vein and exteriorized through the back of the neck. The catheters were kept patent with heparin sodium (10 IU/ml, Pfizer) and sealed with a stainless steel plug. Mice were allowed 4—5 days postsurgical recovery. Food pellets were placed at the bottom of the cage to facilitate recovery. Body weight was recorded daily, and mice that had less than 5% weight loss were subsequently studied.

Hyperinsulinemic euglycemic clamps were performed on 6 h fasted, conscious, and unrestrained mice. The infusion protocol consisted of a 60 min tracer equilibration period ($t = -60$ to 0 min), followed by a 120 min experimental period ($t = 0—120$ min). A bolus of [3-^{3}H] glucose (2.5 μCi; PerkinElmer) was administered at $t = -60$ min, followed by a constant infusion of 0.05 μCi/min for 60 min, starting at 0900 h. At $t = -15$ and -5 min, blood samples (~50 μl) were obtained from a small nick in the tail vein for the assessment of basal plasma glucose concentration, plasma insulin, and glucose-specific activity. At 1000 h, hyperinsulinemic, euglycemic clamp was initiated at $t = 0$ min with an infusion of human insulin (4 mU/kg/min; ActRapid; Novo Nordisk). To minimize changes in glucose specific activity, the continuous infusion of high-pressure liquid chromatography-purified [3-^{3}H]glucose was increased to 0.1 μCi/min and maintained throughout the procedure. Blood glucose was measured every 5 min, and 30% dextrose (3 g of D(+)-Glucose in 10 ml of saline, Merck) was infused at variable rates to maintain euglycemia (~6.5—7.5 mmol/L). Blood samples (10 μl) were taken every 10 min from $t = 90—120$ min to determine glucose-specific activity. At the end of the clamp procedure, mice were anesthetized with sodium pentobarbital (60 mg/kg), tissues were extracted within minutes and stored in −80 °C for later analysis. Plasma insulin was determined from samples obtained from cardiac puncture.

4.11. Determination of plasma and tissue radioactivity

Blood samples (10 μl) were deproteinized with equal molar volume (0.3N) of barium hydroxide and zinc sulfate. [3-^{3}H]glucose radioactivity in the supernatant was assessed by liquid scintillation counting. Whole body glucose kinetics, such as the rate of glucose appearance (endogenous R_a) and disappearance (R_d), were calculated using isotopic steady-state equations of Steel. Endogenous glucose production during the clamp was calculated by subtracting the glucose infusion rate (GIR) from whole body R_d. The insulin-stimulated component of the R_d (IS-R_d) is equal to clamp R_d minus the basal glucose turnover rate. 2 [^{14}C]DG radioactivity was determined by liquid scintillation counting. Soleus, extensor digitorum longus, gastrocnemius, kidney, WAT, BAT, and heart lysates were processed through ion-exchange chromatography columns (Poly-Prep Prefilled Chromatography Columns, AG1-X8 resin, 100—200 mesh dry; Bio-Rad) to separate 2DG from 2DG-6-phosphate (2DG6P). The area under the tracer disappearance curve of [^{14}C]2DG and the radioactivity for the phosphorylated [^{14}C]2DG from individual tissues were used to calculate the glucose metabolic index (Rg′).

4.12. Blockade of MC4R by AgRP

Mice were cannulated for icv injections as described previously [33]. One hour before the start of saline or α-MSH infusion, AgRP (1.0 nmol, 1 μl) or aCSF (1 μl) was injected into the lateral ventricle. The dose of AgRP was selected from pilot experiments, which showed that 1.0 nmol of icv AgRP(83-132) completely blocked the anorectic effect of 1.0 nmol of MTII (a high affinity melanocortin receptor agonist) when is injected 1 h before MTII. A similar dose (0.2—1.0 nmol) was used previously to block central MC3/4 receptors [59].

4.13. Passive administration of polyclonal neutralizing α-MSH IgG

Mice fed a regular diet were matched in their weight and in their glucose values during GTT. After 3 h of fasting, mice received an iv injection of 200 μl of anti α-MSH (20 μg/ml, Sigma). This concentration corresponds to 100 times molar excess to of normal α-MSH levels in humans (~50 pM), This quantity of antibody is able to bind 100% of α-MSH in circulation as was previously demonstrated to neutralizing others peptides [60]. Ninety min after antibody injection, basal glucose was measured and GTT was performed as described. As a control, a group of mice was injected with an equal amount of purified rabbit IgG (Zymed, Life technologies). To evaluate a potential nonspecific effect of the antibody on glucose levels, a week before the immunoneutralization experiment, mice received an iv injection of 200 μl of saline and glucose levels were measured. Another group of mice were cannulated for icv injections and anti α-MSH (10 μg/ml, 1 μl) or purified rabbit IgG (1 μl) was injected into the lateral ventricle. The specificity of injected antibodies were evaluated by incubation of serum from the mice treated either with anti α-MSH or rabbit IgG with ^{125}I-α-MSH.

4.14. Passive administration of MC5R antagonist

A highly selective and potent MC5R antagonist was synthesized according to the structure (Peptide code 5) previously published [21]. After an overnight fast, mice received an intraperitoneal injection of either saline or MC5R antagonist (4 nmol/l, 100 μl) 15 min before glucose challenge.

4.15. α-MSH immunoassay

In plasma and tissues were measured by an in-house radioimmunoassay using a rabbit anti-α-MSH (#M0939). In previous publications, we validated this RIA to use in human, non-human primates and mouse plasma [32,33]. Briefly, considering that α-MSH is a tridecapeptide with an amino acids sequence that is identical to residues 1—13 of ACTH and that only differs in the N-terminal acetyl and C-terminal valine-amide, we performed a displacement technique to test the cross reactivity of the anti-α-MSH antibody with ACTH. We found that the anti-α-MSH antibody cannot detect ACTH in the concentration studied (10—100 pg/ml). Similarly to ACTH, we did not find any cross reaction between α-MSH and β-and γ-MSH [33]. Furthermore, to demonstrate that α-MSH detected in plasma is not a degradation product of ACTH, we added ACTH to human pool of plasma and endogenous α-MSH and ACTH, which was measured during 24 h at 25 °C. Although ACTH degraded at room temperature no increase of α-MSH as a degradation product was detected [32].

4.16. ACTH immunoassay

Plasma ACTH levels were measured by a commercially available IRMA (IRMA ACTH, Mitsubishi Kagaku Iatron, Inc, Tokyo, Japan) as was previously described [32]. According to manufacturer, the antibody does not cross react with α-MSH, or ACTH 1-24, but it can detect human and rat ACTH 1-39.

4.17. Statistical analysis

All values are expressed as mean ± SEM. Group mean differences were assessed using Student's unpaired t-test when two groups were compared. AUC was calculated by trapezoid analysis and was compared by t-test. Data were analyzed by one-way or two-way analysis of variance (ANOVA) followed by Bonferroni's multiple-comparison post hoc test when more of two groups were compared or for time courses or dose response studies. Correlation was analyzed by linear regression analysis. $p < 0.05$ was considered statistically significant. Analyses were performed with GraphPad Prism 6.0 (GraphPad Software, Inc.).

AUTHOR CONTRIBUTIONS

PJE, WC and MAC conceived of the project, designed and performed the majority of the experiments. PJE, WC and MAC wrote and edited the manuscript. PJE and MAC coordinated the collaborations. MCGR performed the majority of cell culture and *in vitro* experiments, contributed to the experimental design and wrote the manuscript. AEE contributed to the experimental design and performed studies in monkeys and mice. SMC, BEG, coordinated and performed monkey's experiments. UG, HLM, TR, CLR provided human studies and patient samples. BAH and IJC performed all studies in sheep. RDB, SAS, SAL SL and SM performed *in vivo* experiment in mice. CB assisted with *in vivo* infusions. SLM, MHT and MJ performed seahorse studies. MJW assisted with *in vitro* experiments. KLG coordinated the primate studies and contributed to the experimental design.

FUNDING

This work was supported by grants from Veski, Monash University, Pfizer Australia, NH&MRC of Australia 606662, the National Heart Foundation of Australia, the US National Institutes of Health RR0163 and DK62202.

ACKNOWLEDGMENTS

We thank CL Møller and BS Wulff for the useful discussions and suggestions with the agonist and antagonist studies in cells, BB Lowell (Harvard Medical School) for POMC-mutKIR6.2 mice and RL Mynatt (Lousiana State University) for MC5R KO mice and J Pagnon for technical assistance.

COMPETING INTERESTS

The authors declared that no conflict of interest exists.

APPENDIX A. SUPPLEMENTARY DATA

Supplementary data related to this article can be found at http://dx.doi.org/10.1016/j.molmet.2016.07.009.

REFERENCES

[1] Raffin-Sanson, M.L., de Keyzer, Y., Bertagna, X., 2003. Proopiomelanocortin, a polypeptide precursor with multiple functions: from physiology to pathological conditions. European Journal of Endocrinology 149(2):79—90. PubMed PMID: 12887283.

[2] Cone, R.D., 2006. Studies on the physiological functions of the melanocortin system. Endocrine Reviews 27(7):736—749. http://dx.doi.org/10.1210/er.2006-0034 [Epub 2006/11/02]. PubMed PMID: 17077189.

[3] Budry, L., Lafont, C., El Yandouzi, T., Chauvet, N., Conejero, G., Drouin, J., et al., 2011. Related pituitary cell lineages develop into interdigitated 3D cell networks. Proceedings of the National Academy of Sciences of the United States of America 108(30):12515–12520. http://dx.doi.org/10.1073/pnas.1105929108. PubMed PMID: 21746936; PubMed Central PMCID: PMCPMC3145718.

[4] Gibson, S., Crosby, S.R., Stewart, M.F., Jennings, A.M., McCall, E., White, A., 1994. Differential release of proopiomelanocortin-derived peptides from the human pituitary: evidence from a panel of two-site immunoradiometric assays. Journal of Clinical Endocrinology & Metabolism 78(4):835–841. http://dx.doi.org/10.1210/jcem.78.4.8157708. PubMed PMID: 8157708.

[5] Zelent, D., Golson, M.L., Koeberlein, B., Quintens, R., van Lommel, L., Buettger, C., et al., 2006. A glucose sensor role for glucokinase in anterior pituitary cells. Diabetes 55(7):1923–1929. PubMed PMID: 16804059.

[6] An, J.J., Rhee, Y., Kim, S.H., Kim, D.M., Han, D.H., Hwang, J.H., et al., 2007. Peripheral effect of alpha-melanocyte-stimulating hormone on fatty acid oxidation in skeletal muscle. Journal of Biological Chemistry 282(5):2862–2870. http://dx.doi.org/10.1074/jbc.M603454200. PubMed PMID: 17127674.

[7] Fan, W., Dinulescu, D.M., Butler, A.A., Zhou, J., Marks, D.L., Cone, R.D., 2000. The central melanocortin system can directly regulate serum insulin levels. Endocrinology 141(9):3072–3079. http://dx.doi.org/10.1210/endo.141.9.7665 [Epub 2000/08/31]. PubMed PMID: 10965876.

[8] Obici, S., Feng, Z., Tan, J., Liu, L., Karkanias, G., Rossetti, L., 2001. Central melanocortin receptors regulate insulin action. The Journal of Clinical Investigation 108(7):1079–1085. http://dx.doi.org/10.1172/JCI12954. PubMed PMID: 11581309; PubMed Central PMCID: PMC200952.

[9] Costa, J.L., Hochgeschwender, U., Brennan, M., 2006. The role of melanocyte-stimulating hormone in insulin resistance and type 2 diabetes mellitus. Treat Endocrinol 5(1):7–13. PubMed PMID: 16396514.

[10] Katsuki, A., Sumida, Y., Murashima, S., Furuta, M., Araki-Sasaki, R., Tsuchihashi, K., et al., 2000. Elevated plasma levels of alpha-melanocyte stimulating hormone (alpha-MSH) are correlated with insulin resistance in obese men. International Journal of Obesity and Related Metabolic Disorders 24(10):1260–1264. PubMed PMID: 11093286.

[11] Hoggard, N., Johnstone, A.M., Faber, P., Gibney, E.R., Elia, M., Lobley, G., et al., 2004. Plasma concentrations of alpha-MSH, AgRP and leptin in lean and obese men and their relationship to differing states of energy balance perturbation. Clinical Endocrinology (Oxford) 61(1):31–39. http://dx.doi.org/10.1111/j.1365-2265.2004.02056.x. PubMed PMID: 15212642.

[12] Zurlo, F., Larson, K., Bogardus, C., Ravussin, E., 1990. Skeletal muscle metabolism is a major determinant of resting energy expenditure. Journal of Clinical Investigation 86(5):1423–1427. http://dx.doi.org/10.1172/JCI114857 [Epub 1990/11/01]. PubMed PMID: 2243122; PubMed Central PMCID: PMC296885.

[13] Ferrannini, E., 1998. Insulin resistance versus insulin deficiency in non-insulin-dependent diabetes mellitus: problems and prospects. Endocrine Reviews 19(4):477–490. PubMed PMID: 9715376.

[14] Saloranta, C., Groop, L., 1996. Interactions between glucose and FFA metabolism in man. Diabetes Metabolism Reviews 12(1):15–36. http://dx.doi.org/10.1002/(SICI)1099-0895(199603)12:1<15::AID-DMR153>3.0.CO;2-0. PubMed PMID: 8861499.

[15] Parton, L.E., Ye, C.P., Coppari, R., Enriori, P.J., Choi, B., Zhang, C.Y., et al., 2007. Glucose sensing by POMC neurons regulates glucose homeostasis and is impaired in obesity. Nature 449(7159):228–232. http://dx.doi.org/10.1038/nature06098 [Epub 2007/08/31]. nature06098 [pii]. PubMed PMID: 17728716.

[16] Badin, P.M., Vila, I.K., Louche, K., Mairal, A., Marques, M.A., Bourlier, V., et al., 2013. High-fat diet-mediated lipotoxicity and insulin resistance is related to impaired lipase expression in mouse skeletal muscle. Endocrinology 154(4):1444–1453. http://dx.doi.org/10.1210/en.2012-2029 [Epub 2013/03/09]. en.2012-2029 [pii]. PubMed PMID: 23471217.

[17] Henry, B.A., Dunshea, F.R., Gould, M., Clarke, I.J., 2008. Profiling postprandial thermogenesis in muscle and fat of sheep and the central effect of leptin administration. Endocrinology 149(4):2019–2026. http://dx.doi.org/10.1210/en.2007-1311. PubMed PMID: 18162524.

[18] Grieco, P., Lavecchia, A., Cai, M., Trivedi, D., Weinberg, D., MacNeil, T., et al., 2002. Structure-activity studies of the melanocortin peptides: discovery of potent and selective affinity antagonists for the hMC3 and hMC4 receptors. Journal of Medicinal Chemistry 45(24):5287–5294 [Epub 2002/11/15]. jm0202526 [pii]. PubMed PMID: 12431055.

[19] Moller, C.L., Raun, K., Jacobsen, M.L., Pedersen, T.A., Holst, B., Conde-Frieboes, K.W., et al., 2011. Characterization of murine melanocortin receptors mediating adipocyte lipolysis and examination of signalling pathways involved. Molecular and Cellular Endocrinology 341(1–2):9–17. http://dx.doi.org/10.1016/j.mce.2011.03.010. PubMed PMID: 21616121.

[20] Chen, W., Kelly, M.A., Opitz-Araya, X., Thomas, R.E., Low, M.J., Cone, R.D., 1997. Exocrine gland dysfunction in MC5-R-deficient mice: evidence for coordinated regulation of exocrine gland function by melanocortin peptides. Cell 91(6):789–798 [Epub 1997/12/31]. PubMed PMID: 9413988.

[21] Balse-Srinivasan, P., Grieco, P., Cai, M., Trivedi, D., Hruby, V.J., 2003. Structure-activity relationships of novel cyclic alpha-MSH/beta-MSH hybrid analogues that lead to potent and selective ligands for the human MC3R and human MC5R. Journal of Medicinal Chemistry 46(17):3728–3733. http://dx.doi.org/10.1021/jm030111j. PubMed PMID: 12904077.

[22] Catania, A., Gatti, S., Colombo, G., Lipton, J.M., 2004. Targeting melanocortin receptors as a novel strategy to control inflammation. Pharmacological Reviews 56(1):1–29. http://dx.doi.org/10.1124/pr.56.1.1 [Epub 2004/03/06]. 56/1/1 [pii]. PubMed PMID: 15001661.

[23] Zhu, J., Mix, E., Winblad, B., 2001. The antidepressant and antiinflammatory effects of rolipram in the central nervous system. CNS Drug Reviews 7(4):387–398 [Epub 2002/02/07]. PubMed PMID: 11830756.

[24] Cakir, M., Sari, R., Tosun, O., Karayalcin, U., 2005. Cortisol levels during an oral glucose tolerance test in lean and obese women. Endocrine Research 31(3):213–218 [Epub 2006/01/06]. PubMed PMID: 16392623.

[25] Catania, A., Airaghi, L., Colombo, G., Lipton, J.M., 2000. Alpha-melanocyte-stimulating hormone in normal human physiology and disease states. Trends in Endocrinology and Metabolism: TEM 11(8):304–308. PubMed PMID: 10996524.

[26] Kumar, T.C., Vincent, D.S., 1974. Fine structure of the pars intermedia in the rhesus monkey, Macaca mulatta. Journal of Anatomy 118(Pt 1):155–169. PubMed PMID: 4372205.

[27] Coates, P.J., Doniach, I., Hale, A.C., Rees, L.H., 1986. The distribution of immunoreactive alpha-melanocyte-stimulating hormone cells in the adult human pituitary gland. Journal of Endocrinology 111(2):335–342. PubMed PMID: 3025327.

[28] Evans, V.R., Manning, A.B., Bernard, L.H., Chronwall, B.M., Millington, W.R., 1994. Alpha-melanocyte-stimulating hormone and N-acetyl-beta-endorphin immunoreactivities are localized in the human pituitary but are not restricted to the zona intermedia. Endocrinology 134(1):97–106. PubMed PMID: 8275975.

[29] Yamashita, M., Sano, T., Qian, Z.R., Kovacs, K., Horvath, E., 2006. Diversity of ACTH-immunoreactive cells in the human adenohypophysis: an immunohistochemical study with special reference to cluster formation and follicular cell association. Endocrine Pathology 17(2):155–164. PubMed PMID: 17159248.

[30] Matejec, R., Locke, G., Muhling, J., Harbach, H.W., Langefeld, T.W., Bodeker, R.H., et al., 2009. Release of melanotroph- and corticotroph-type proopiomelanocortin derivatives into blood after administration of corticotropin-releasing hormone in patients with septic shock without adrenocortical insufficiency. Shock 31(6):553–560. http://dx.doi.org/10.1097/SHK.0b013e318188dfb8 [Epub 2008/10/02]. PubMed PMID: 18827746.

[31] Donahoo, W.T., Hernandez, T.L., Costa, J.L., Jensen, D.R., Morris, A.M., Brennan, M.B., et al., 2009. Plasma alpha-melanocyte-stimulating hormone: sex differences and correlations with obesity. Metabolism 58(1):16–21. http://dx.doi.org/10.1016/j.metabol.2008.07.028. PubMed PMID: 19059526.

[32] Roth, C.L., Enriori, P.J., Gebhardt, U., Hinney, A., Muller, H.L., Hebebrand, J., et al., 2010. Changes of peripheral alpha-melanocyte-stimulating hormone in childhood obesity. Metabolism 59(2):186–194. http://dx.doi.org/10.1016/j.metabol.2009.06.031 [Epub 2009/09/22]. S0026-0495(09)00302-3 [pii]. PubMed PMID: 19766264.

[33] Enriori, P.J., Evans, A.E., Sinnayah, P., Jobst, E.E., Tonelli-Lemos, L., Billes, S.K., et al., 2007. Diet-induced obesity causes severe but reversible leptin resistance in arcuate melanocortin neurons. Cell Metabolism 5(3):181–194. http://dx.doi.org/10.1016/j.cmet.2007.02.004 [Epub 2007/03/07]. S1550-4131(07)00036-8 [pii]. PubMed PMID: 17339026.

[34] Beer, S.F., Bircham, P.M., Bloom, S.R., Clark, P.M., Hales, C.N., Hughes, C.M., et al., 1989. The effect of a 72-h fast on plasma levels of pituitary, adrenal, thyroid, pancreatic and gastrointestinal hormones in healthy men and women. Journal of Endocrinology 120(2):337–350. PubMed PMID: 2926306.

[35] Giovannini, C., Ciucci, E., Clementi, R., Cugini, P., Facchinetti, F., Negri, M., 1990. Beta-endorphin, insulin, ACTH and cortisol plasma levels during oral glucose tolerance test in obesity after weight loss. Hormone and Metabolic Research 22(2):96–100. http://dx.doi.org/10.1055/s-2007-1004859. PubMed PMID: 2157655.

[36] Balon-Perin, S., Kolanowski, J., Berbinschi, A., Franchimont, P., Ketelslegers, J.M., 1991. The effects of glucose ingestion and fasting on plasma immunoreactive beta-endorphin, adrenocorticotropic hormone and cortisol in obese subjects. Journal of Endocrinological Investigation 14(11):919–925. http://dx.doi.org/10.1007/BF03347116. PubMed PMID: 1666898.

[37] Nogueiras, R., Wiedmer, P., Perez-Tilve, D., Veyrat-Durebex, C., Keogh, J.M., Sutton, G.M., et al., 2007. The central melanocortin system directly controls peripheral lipid metabolism. Journal of Clinical Investigation 117(11):3475–3488. http://dx.doi.org/10.1172/JCI31743 [Epub 2007/09/22]. PubMed PMID: 17885689; PubMed Central PMCID: PMC1978426.

[38] Toda, C., Shiuchi, T., Lee, S., Yamato-Esaki, M., Fujino, Y., Suzuki, A., et al., 2009. Distinct effects of leptin and a melanocortin receptor agonist injected into medial hypothalamic nuclei on glucose uptake in peripheral tissues. Diabetes 58(12):2757–2765. http://dx.doi.org/10.2337/db09-0638 [Epub 2009/09/16]. db09-0638 [pii]. PubMed PMID: 19752162; PubMed Central PMCID: PMC2780865.

[39] Hochgeschwender, U., Costa, J.L., Reed, P., Bui, S., Brennan, M.B., 2003. Altered glucose homeostasis in proopiomelanocortin-null mouse mutants lacking central and peripheral melanocortin. Endocrinology 144(12):5194–5202. http://dx.doi.org/10.1210/en.2003-1008 [Epub 2003/09/13]. PubMed PMID: 12970157.

[40] Aslan, I.R., Ranadive, S.A., Valle, I., Kollipara, S., Noble, J.A., Vaisse, C., 2013. The melanocortin system and insulin resistance in humans: insights from a patient with complete POMC deficiency and type 1 diabetes mellitus. International Journal of Obesity (London). http://dx.doi.org/10.1038/ijo.2013.53 [Epub 2013/05/08]. ijo201353 [pii]. PubMed PMID: 23649472.

[41] Gavrila, A., Chan, J.L., Miller, L.C., Heist, K., Yiannakouris, N., Mantzoros, C.S., 2005. Circulating melanin-concentrating hormone, agouti-related protein, and alpha-melanocyte-stimulating hormone levels in relation to body composition: alterations in response to food deprivation and recombinant human leptin administration. Journal of Clinical Endocrinology & Metabolism 90(2):1047–1054. http://dx.doi.org/10.1210/jc.2004-1124. PubMed PMID: 15546902.

[42] Forbes, S., Bui, S., Robinson, B.R., Hochgeschwender, U., Brennan, M.B., 2001. Integrated control of appetite and fat metabolism by the leptin-proopiomelanocortin pathway. Proceedings of the National Academy of Sciences of the United States of America 98(7):4233–4237. PubMed PMID: 11259669.

[43] Tanaka, T., Masuzaki, H., Yasue, S., Ebihara, K., Shiuchi, T., Ishii, T., et al., 2007. Central melanocortin signaling restores skeletal muscle AMP-activated protein kinase phosphorylation in mice fed a high-fat diet. Cell Metabolism 5(5):395–402. http://dx.doi.org/10.1016/j.cmet.2007.04.004 [Epub 2007/05/10]. S1550-4131(07)00099-X [pii]. PubMed PMID: 17488641.

[44] Fathi, Z., Iben, L.G., Parker, E.M., 1995. Cloning, expression, and tissue distribution of a fifth melanocortin receptor subtype. Neurochemical Research 20(1):107–113 [Epub 1995/01/01]. PubMed PMID: 7739752.

[45] Morgan, C., Cone, R.D., 2006. Melanocortin-5 receptor deficiency in mice blocks a novel pathway influencing pheromone-induced aggression. Behavior Genetics 36(2):291–300. http://dx.doi.org/10.1007/s10519-005-9024-9 [Epub 2006/01/13]. PubMed PMID: 16408249.

[46] Valli-Jaakola, K., Suviolahti, E., Schalin-Jantti, C., Ripatti, S., Silander, K., Oksanen, L., et al., 2008. Further evidence for the role of ENPP1 in obesity: association with morbid obesity in Finns. Obesity (Silver Spring) 16(9):2113–2119. http://dx.doi.org/10.1038/oby.2008.313 [Epub 2008/06/14]. oby2008313 [pii]. PubMed PMID: 18551113.

[47] Sutton, G.M., Begriche, K., Kumar, K.G., Gimble, J.M., Perez-Tilve, D., Nogueiras, R., et al., 2010. Central nervous system melanocortin-3 receptors are required for synchronizing metabolism during entrainment to restricted feeding during the light cycle. FASEB Journal : Official Publication of the Federation of American Societies for Experimental Biology 24(3):862–872. http://dx.doi.org/10.1096/fj.09-142000 [Epub 2009/10/20]. PubMed PMID: 19837866; PubMed Central PMCID: PMC2830138.

[48] Albarado, D.C., McClaine, J., Stephens, J.M., Mynatt, R.L., Ye, J., Bannon, A.W., et al., 2004. Impaired coordination of nutrient intake and substrate oxidation in melanocortin-4 receptor knockout mice. Endocrinology 145(1):243–252. http://dx.doi.org/10.1210/en.2003-0452 [Epub 2003/10/11]. en.2003-0452 [pii]. PubMed PMID: 14551222.

[49] Kumar, K.G., Sutton, G.M., Dong, J.Z., Roubert, P., Plas, P., Halem, H.A., et al., 2009. Analysis of the therapeutic functions of novel melanocortin receptor agonists in MC3R- and MC4R-deficient C57BL/6J mice. Peptides 30(10):1892–1900. http://dx.doi.org/10.1016/j.peptides.2009.07.012 [Epub 2009/08/04]. S0196-9781(09)00303-9 [pii]. PubMed PMID: 19646498; PubMed Central PMCID: PMC2755620.

[50] Rodrigues, A.R., Pignatelli, D., Almeida, H., Gouveia, A.M., 2009. Melanocortin 5 receptor activates ERK1/2 through a PI3K-regulated signaling mechanism. Molecular and Cellular Endocrinology 303(1–2):74–81. http://dx.doi.org/10.1016/j.mce.2009.01.014 [Epub 2009/05/12]. S0303-7207(09)00063-X [pii]. PubMed PMID: 19428994.

[51] Kanda, Y., Watanabe, Y., 2007. Adrenaline increases glucose transport via a Rap1-p38MAPK pathway in rat vascular smooth muscle cells. British Journal of Pharmacology 151(4):476–482. http://dx.doi.org/10.1038/sj.bjp.0707247 [Epub 2007/04/24]. 0707247 [pii]. PubMed PMID: 17450172; PubMed Central PMCID: PMC2013965.

[52] Jessen, N., An, D., Lihn, A.S., Nygren, J., Hirshman, M.F., Thorell, A., et al., 2011. Exercise increases TBC1D1 phosphorylation in human skeletal muscle. American Journal of Physiology. Endocrinology and Metabolism 301(1):E164–E171. http://dx.doi.org/10.1152/ajpendo.00042.2011. PubMed PMID: 21505148; PubMed Central PMCID: PMCPMC3129834.

[53] Stuart, C.A., Howell, M.E., Zhang, Y., Yin, D., 2009. Insulin-stimulated translocation of glucose transporter (GLUT) 12 parallels that of GLUT4 in normal muscle. Journal of Clinical Endocrinology & Metabolism 94(9):3535–3542. http://dx.doi.org/10.1210/jc.2009-0162. PubMed PMID: 19549745; PubMed Central PMCID: PMCPMC2741719.

[54] Conti, M., Beavo, J., 2007. Biochemistry and physiology of cyclic nucleotide phosphodiesterases: essential components in cyclic nucleotide signaling. Annual Review of Biochemistry 76:481–511. http://dx.doi.org/10.1146/annurev.biochem.76.060305.150444 [Epub 2007/03/23]. PubMed PMID: 17376027.

[55] Wouters, E.F., Bredenbroker, D., Teichmann, P., Brose, M., Rabe, K.F., Fabbri, L.M., et al., 2012. Effect of the phosphodiesterase 4 inhibitor roflumilast on glucose metabolism in patients with treatment-naive, newly diagnosed type 2 diabetes mellitus. Journal of Clinical Endocrinology & Metabolism 97(9):E1720–E1725. http://dx.doi.org/10.1210/jc.2011-2886 [Epub 2012/06/23]. PubMed PMID: 22723325.

[56] Luquet, S., Perez, F.A., Hnasko, T.S., Palmiter, R.D., 2005. NPY/AgRP neurons are essential for feeding in adult mice but can be ablated in neonates. Science 310(5748):683–685. PubMed PMID: 16254186.

[57] Koegler, F.H., Enriori, P.J., Billes, S.K., Takahashi, D.L., Martin, M.S., Clark, R.L., et al., 2005. Peptide YY(3-36) inhibits morning, but not evening, food intake and decreases body weight in rhesus macaques. Diabetes 54(11): 3198–3204 [Epub 2005/10/27]. 54/11/3198 [pii]. PubMed PMID: 16249445.

[58] McCurdy, C.E., Bishop, J.M., Williams, S.M., Grayson, B.E., Smith, M.S., Friedman, J.E., et al., 2009. Maternal high-fat diet triggers lipotoxicity in the fetal livers of nonhuman primates. Journal of Clinical Investigation 119(2): 323–335. http://dx.doi.org/10.1172/JCI32661 [Epub 2009/01/17]. 32661 [pii]. PubMed PMID: 19147984; PubMed Central PMCID: PMC2631287.

[59] Enriori, P.J., Sinnayah, P., Simonds, S.E., Garcia Rudaz, C., Cowley, M.A., 2011. Leptin action in the dorsomedial hypothalamus increases sympathetic tone to brown adipose tissue in spite of systemic leptin resistance. Journal of Neuroscience 31(34):12189–12197. http://dx.doi.org/10.1523/JNEUROSCI.2336-11.2011 [Epub 2011/08/26]. 31/34/12189 [pii]. PubMed PMID: 21865462.

[60] Sugimoto, H., Hamano, Y., Charytan, D., Cosgrove, D., Kieran, M., Sudhakar, A., et al., 2003. Neutralization of circulating vascular endothelial growth factor (VEGF) by anti-VEGF antibodies and soluble VEGF receptor 1 (sFlt-1) induces proteinuria. Journal of Biological Chemistry 278(15):12605–12608. http://dx.doi.org/10.1074/jbc.C300012200 [Epub 2003/01/23]. C300012200 [pii]. PubMed PMID: 12538598.

